

Re-assessing the European lithium resource potential – A review of *hard-rock* resources and metallogeny

B. Gourcerol^{a,b,*}, E. Gloaguen^{b,c}, J. Melletton^b, J. Tuduri^b, Xavier Galiegue^a

^a Laboratoire d'Economie d'Orléans, Université d'Orléans, UMR7322 Faculté de Droit d'Economie et de Gestion Rue de Blois, BP 26739 45067 Orleans Cedex 2, France

^b BRGM, F-45060 Orléans, France

^c ISTO, UMR 7327, Université d'Orléans, CNRS, BRGM, F-45071 Orléans, France

ARTICLE INFO

Keywords:
Lithium
Metallogeny
Pegmatite
Europe
Resources

ABSTRACT

Lithium, which is an excellent conductor of heat and electricity, became a strategic metal in the past decade due to its widespread use in electromobility and green technologies. The resulting significant increase in demand has revived European interest in lithium mining, leading several countries to assess their own resources/reserves in order to secure their supplies. In this context, we present for the first time a geographically-based and geological compilation of European lithium *hard-rock* occurrences and deposits with their corresponding features (e.g., deposit types, Li-bearing minerals, Li concentrations), as well as a systematic assessment of metallogenetic processes related to lithium mineralization. It appears that lithium is well represented in various deposit types related to several orogenic cycles from Precambrian to Miocene ages. About thirty hard-rock deposits have been identified, mostly resulting from endogenous processes such as lithium-cesium-tantalum (LCT) pegmatites (e.g., Sepeda in Portugal, Aclare in Ireland, Läntta in Finland), rare-metal granites (RMG; Beauvoir in France, Cinovec in the Czech Republic) and greisen (Cligga Head, Tregonning-Godolphin, Meldon in the UK and Montebras in France). Local exogenous processes may result in significant Li-enrichment, such as jadarite precipitation in the Jadar Basin (Serbia), but they are rarely related to economic lithium grades such as in Mn-(Fe) deposits, or in bauxite. We also identified major common parameters leading to Li enrichment: 1) a pre-existing Li-bearing source; 2) the presence of lithospheric thickening, which may be a favorable process for concentrating Li; 3) a regional or local extensional regime; and 4) the existence of fractures acting as channel ways for exogenous processes. Furthermore, we point out the heterogeneity of knowledge for several orogenic settings, such as the Mediterranean orogens, suggesting either a lack of exploration in this geographical area, or significant changes in the orogenic parameters.

1. Introduction

Over the past decade, lithium has become a strategic metal due to its physical and chemical properties, being the lightest solid element and an excellent conductor of heat and electricity. This makes it an excellent candidate for electromobility and green technologies, such as Li-ion batteries and other energy-storage devices (Armand and Tarascon, 2008; Tarascon, 2010; Ziemann et al., 2012; Manthiram et al., 2017). As a result, Li demand has increased significantly and a “lithium rush” is currently happening world wide (e.g., Roskill Information Services Ltd., 2016). In this context, the identification and assessment of lithium mineral resources and -reserves is a crucial step, as is understanding lithium metallogeny, a major subject for discovering new mineral resources.

Historically, two distinct deposit types are identified: 1) *brine* deposits in which the lithium grade is about 0.1% Li₂O; and 2) *hard-rock* deposits

where the lithium grade generally varies from 0.6 to 1.0% Li₂O hosted by various Li-bearing minerals (Kesler et al., 2012; Mohr et al., 2012).

The brine-deposit type refers to relatively recent (mostly Quaternary), enclosed, tectonically active basins that contain Li-rich lacustrine evaporites. These are produced by high evaporation rates in an arid to hyper-arid climate and/or by various water inputs such as groundwater and spring water circulation (e.g., Erickson and Salas, 1987; Bradley et al., 2013). In these deposits, the Li source and enrichment processes are specific to each brine. However, the most accepted model is the weathering of felsic rocks and/or local hydrothermal activity driven by a magmatic heat source through active channel pathways (Bradley et al., 2013; Hofstra et al., 2013). In North America, several deposits have been identified within the Basin and Range extensional province of the western United States, including the Clayton Valley and the Great Salt Lake (e.g., Bradley et al., 2013). In South America and more particularly on the Puna Plateau,

* Corresponding author at: BRGM, F-45060 Orléans, France.

E-mail address: b.gourcerol@brgm.fr (B. Gourcerol).

Table 1

Main Li-bearing minerals encountered in Europe, their corresponding chemical formula, Li content and physical characteristics.

Name	Formula	Mineral group	Theoretical values		Specific gravity (g/cm ³)	Hardness
			Li ₂ O %	Li metal %		
Eucryptite	LiAlSiO ₄	Feldspathoid	11.86	5.51	2.67	6.5
Amblygonite	(Li,Na)Al(PO ₄)(F,OH)	Phosphate	10.1	4.69	2.98	5.5–6
Montebrasite	LiAl(PO ₄)(OH,F)	Phosphate	10.1	4.69	3.98	5.5–7
Lithiophilite	Li(Mn,Fe)PO ₄	Phosphate	9.53	4.43	3.5	5
Sicklerite	Li _{1-x} (Fe ³⁺ , Mn ²⁺) _x PO ₄	Phosphate	< 9.48	4.40	3.2–3.4	4
Ferrisicklerite	Li _{1-x} (Fe ³⁺ , Mn ²⁺) _x PO ₄	Phosphate	< 9.47	4.40	3.2–3.4	4
Triphylite	Li(Fe,Mn)PO ₄	Phosphate	9.47	4.40	3.5	4–5
Spodumene	LiAl(Si ₂ O ₆)	Inosilicate	8.03	3.73	3.2	6.5–7
Lepidolite	K(Li,Al) ₃ (Si,Al) ₄ O ₁₀ (OH,F) ₂	Phyllosilicate	7.7	3.58	2.8–2.9	1.55–1.59
Jadarite	Li ₂ NaSi ₂ B ₂ O ₇ (OH)	Neosilicate	7.3	3.39	2.45	4–5
Poly lithionite	KLi ₂ Al(Si ₄ O ₁₀)(F,OH) ₂	Phyllosilicate	6.46	3.00	2.58–2.82	2–3
Petalite	LiAl(Si ₄ O ₁₀)	Tectosilicate	4.88	2.26	2.4–2.46	6–6.5
Zinnwaldite	KLiFeAl(Al,Si ₃)O ₁₀ (OH,F) ₂	Phyllosilicate	4.12	1.91	2.9–3.2	5.5–6
Elbaite	Na(Li _{1.5} Al _{1.5})Al ₆ Si ₆ O ₁₈ (BO ₃) ₃ (OH) ₄	Cyclosilicate	4.07	1.89	2.9–3.2	7.5
Holmquistite	X(Li ₂)(Mg ₃ Al ₂)(Si ₈ O ₂₂)(OH) ₂	Inosilicate	3.98	1.85	3.06–3.13	5.5
Cookeite	LiAl ₄ (AlSi ₃ O ₁₀)(OH) ₈	Phyllosilicate	2.9	1.34	2.58–2.69	2.5–3.5
Lithiophorite	(Al,Li)Mn ⁴⁺ O ₂ (OH) ₂	Oxide	1.23	0.57	3.14–3.37	2.5–3

brine deposits, referred to as *salars*, cover an area of about 400,000 km² from northern Argentina and northern Chile to western Bolivia (Erickson and Salas, 1987) named the “lithium triangle”. In this area, several lithium deposits have been identified and are operated by major mining companies including SCL/Chemetall and SQM/Tianqi Lithium Corp. In China, the Qinghai-Tibet plateau is a favorable setting for lithium deposits, as illustrated by the Qaidam (e.g., Shengsong, 1986; Yu et al., 2013) and Zabuye basins, from which some brines are exploited by governmental mining companies.

Hard-rock deposits comprise several styles of Li mineralization in magmatic and/or sedimentary rocks, related to both endogenous (magmatic) and exogenous (re-concentration by weathering, or supergene alteration and transport) processes. They can contain widespread varieties of Li-bearing minerals, such as Li-micas, Li-pyroxenes, Li-silicates, Li-phosphates, etc. (Table 1). Among them, hectorite (Li-bearing clay) from the Kings Valley, Nevada (e.g., Glanzman et al., 1978; Kesler et al., 2012) and jadarite (Li-bearing borosilicate) from Serbia (Stanley et al., 2007; Rio Tinto, 2017; Stojadinovic et al., 2017) represent potential world-class deposits, whereas spodumene-bearing lithium-cesium-tantalum (LCT) pegmatites in the Greenbushes (Australia) have been mined for decades by Talison Lithium Ltd. and others (e.g., Mudd and Jowitt, 2016).

Lithium production historically has been dominated by Australia (e.g., Greenbushes deposits), South America (*Salar de Atacama*) and China (Zabuye, Qaidam Lakes). Thus, of the 36.5 kt Li metal produced in 2016, 39% came from Australia, 32.8% from Chili, 15.6% from Argentina and 5.5% from China. Portugal, the first Li producing European country, represents only 1.3% of world production, especially for the ceramics and glass industry (BRGM, 2017). However, lithium exploration increased significantly (e.g., Roskill Information Services Ltd., 2016), leading other countries in the European Community (France, Austria, Czech Republic, Spain, Finland...) to assess their own mineral resources and –reserves, in order to evaluate their global competitiveness in the lithium industry.

Hereafter, we provide a key to understanding the geological context of lithium in Europe from a hard-rock perspective. To this end, we made a systematic, geographically- and geologically-based compilation of lithium occurrences, significant mineral showings and/or deposits, with their corresponding Li-deposit types, Li-bearing minerals and Li concentrations. For the first time, we present an overview and quantification of identified European Li deposit types and features, and their distribution in the different orogenic settings of Europe. A major effort was made to constrain metallogenetically the Li endowments in order to highlight potential processes (endogenous and exogenous) causing Li enrichment, and to introduce potential prospective regions. The

resulting dataset may be used in future studies for constraining the possible relationships between Li-rich geothermal brines, surficial waters and Li-rich basement rocks.

2. Overview of hard-rock lithium deposit types in Europe

A compilation of lithium occurrences and -deposits was made by collecting information from various geological survey organizations, exploration and mining companies, and scientific research projects and related publications. This resulted in an up-to-date quantification of the European lithium potential, considering only hard-rock ore types, identifying 527 lithium occurrences, projects and deposits (provided as electronic supplementary material). This was almost five times more than the previous Mineral4EU-ProMine (<http://minerals4eu.brgm-rec.fr/>) inventory (Cassard et al., 2015).

In addition, mineral resource and -reserve and -production data were gathered from available published data by exploration and mining companies, such as technical and annual reports, from data repositories (e.g., <https://sedar.com>) and from governmental surveys. Note that the data from England, France and, locally, Germany are based on historical (before 1995), non-compliant CRIRSCO (Committee for Mineral Reserves International Reporting Standards) compliant estimates.

We emphasize that lithium deposits related to seawater, and geothermal- and oilfield brines are not considered in this study.

According to our compilation (and previous ones, e.g., Christmann et al., 2015), two distinct categories of lithium deposits and occurrences are found in Europe. They are: 1) Magmatic-related (Fig. 1A, B, C) deposits; and 2) Sedimentary/hydrothermal-related deposits (Fig. 1D).

2.1. Magmatic-related deposits

2.1.1. Rare-metal granites

Rare-metal granites (RMG; Černý and Ercit, 2005) are felsic, peraluminous to peralkaline intrusive rocks that host magmatic disseminated mineralization. They occur as very small, mostly subsurface, granitic plugs, typically less than 1 km³, such as the Beauvoir RMG in France (Raimbault et al., 1995; Fig. 1A). According to their geochemistry and geodynamic setting, three main types (Linnen and Cuney, 2005; Černý and Ercit, 2005) are recognized:

- 1) Peralkaline RMG have very high contents of F, REE, Y, Zr, Nb, related to anorogenic settings; their Li content is relatively moderate (up to a few 1000 ppm) and is mainly illustrated by zinnwaldite and poly lithionite occurrences (Tables 1 and 2). This type is not documented in Europe;

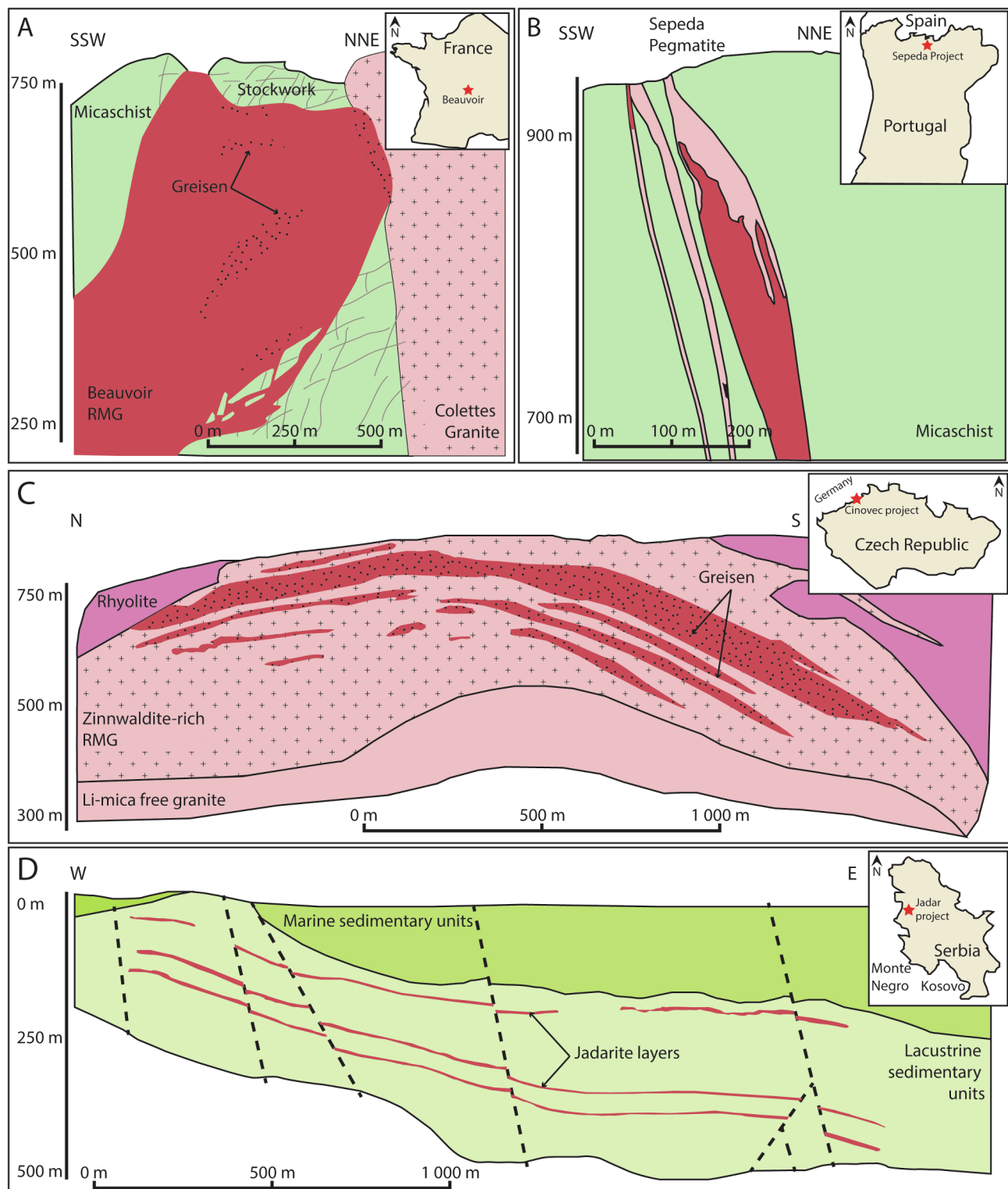


Fig. 1. Cross sections of various lithium deposits. Lithium-bearing units are identified in red in each section. A) Beauvoir RMG (France) and related stockwork (modified from Cuney and Autran, 1987). B) Sepeda pegmatite in Portugal (modified from Dakota Minerals, 2017); pink area represents barren pegmatite. C) Cinovec deposit in Czech Republic (modified from Breiter et al., 2017). D) Jadar Basin in Serbia and location of the jadarite layers (modified from Rio Tinto, 2017). (For interpretation of the references to color in this figure legend, the reader is referred to the web version of this article.)

- 2) Metaluminous to peraluminous, low- to intermediate-phosphorus RMG with high concentrations of Nb, Ta, Sn, that occur in both post- and an-orogenic geodynamic settings. The Li content again is moderate (up to a few 1000 ppm) and is mostly related to zinnwaldite. Examples include Cinovec (Fig. 1C), Podlesí (Fig. 2A), the

Sejby and Homolka granites in the Czech Republic, the Chavence and Les Châtelliers granites in France (Table 2; Černý and Ercit, 2005 and references therein);

- 3) Peraluminous, high-phosphorus RMG with strong enrichment in Ta, Sn, Li and F, occurring in a continental-collision setting. In this RMG

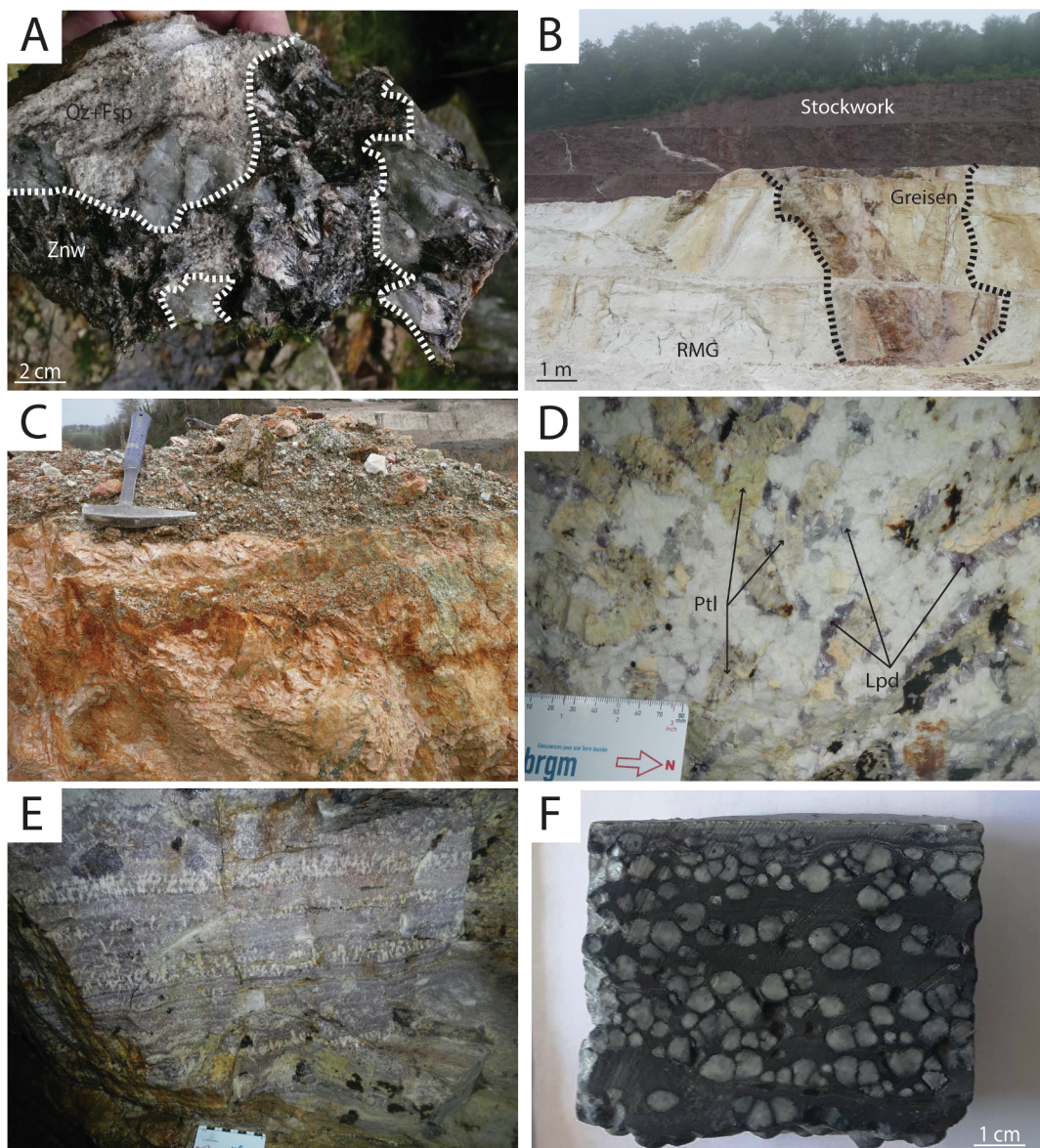


Fig. 2. Photographs of various styles of lithium mineralization. A) Quartz-feldspar and zinnwaldite mineralization (Podlesí, Czech Republic). B) Greisen and related La Bosse stockwork (Beauvoir, Massif Central, France). C) Montebbras stocksheider hosted in RMG (Massif Central, France). D) Phenocrysts of petalite (yellowish-greenish minerals) surrounded by purplish lepidolite in quartz-potassic feldspar-albite matrix (Chédeville pegmatite, Massif Central, France). E) Alternating lepidolite-rich and aplite-rich layers in a horizontal pegmatite (Chédeville pegmatite, Massif Central, France). Scale represents 7 cm. Abbreviations: Lpd: lepidolite; Ptl: petalite; Znw: Zinnwaldite; Qz + Fsp: quartz + feldspar. F) Jadarite mineralization (Jadar Basin, Serbia) in mudstone (courtesy of Matevž Novak, Geological Survey of Slovenia)

type, Li concentrations can be high, from 0.5% to 1.0% Li₂O, and occurring as lepidolite, Li-rich muscovite and amblygonite-monobrasite series, such as at Beauvoir (Fig. 1A, 2B), Montebbras (Fig. 2C) and the Richemont rhyolite dike in the French Massif Central, and Argemela in Portugal (Table 2; Černý and Ercit, 2005 and references therein).

2.1.2. LCT pegmatites

With the exception of some rare giant Precambrian occurrences, lithium-cesium-tantalum (LCT) pegmatites (e.g., London, 2008, 2018; Černý and Ercit, 2005) are relatively small-sized (a few m³ to < 1/2 km³; Fig. 1B), coarse-grained and/or aplitic igneous rocks of granitic composition. Geochemically, Li-rich LCT pegmatites are similar to peraluminous high-phosphorus RMG. They are the result of crystallization of fluid-rich melts, enriched in various amounts of incompatible elements, such as Li, Ta, Sn, Rb, Be, Nb and Cs, and strongly depleted in

REEs, close to chondritic values (London, 1995, 2005, 2008, 2018; Černý and Ercit, 2005; Černý et al., 2012; Linnen et al., 2012).

Pegmatites can form under various P/T conditions (Table 3) representing various classes (e.g., Černý, 1989, 1990; Černý et al., 2012). They are generally clustered in kilometer-size pegmatite fields (e.g., the Ambazac pegmatite field, Deveaud et al., 2013; Silva et al., 2018), and occur as dikes and/or sills (e.g., Emmes pegmatite, Finland, Eilu et al., 2012; Gonçalo pegmatite field, Portugal, Ramos et al., 1994) or lenticular bodies (e.g., Bohemian pegmatites, Melletton et al., 2012). Contacts with host-rock range from relatively sharp to progressive, depending on the nature of the host and the depth of emplacement. Host-rocks are mainly metasedimentary and/or metavolcanic rocks metamorphosed from lower greenschist to amphibolite facies (Černý, 1992) as well as granite intrusions (e.g., Gonçalo, Ambazac).

LCT pegmatites show heterogeneous textures and compositions, and are composed of variable amounts of quartz, plagioclase, potassium

Table 2
RMG classification according to Černý and Ercit (2005) with European examples.

Type	Affinity	Minerals	Favorable setting	Lithium values		Li-bearing minerals	European examples
				Li values	Li ₂ O values		
I	Peralkaline	F, REE, Y, Zr, Nb	Anorogenic	100 to 1 000 ppm	215.27 to 2 152.7 ppm	Zinnwaldite, poly lithionite	NA
II	Metaluminous to peraluminous	Nb, Ta, Sn	Post-orogenic and anorogenic	100 to 1 000 ppm	215.27 to 2 152.7 ppm	Zinnwaldite	Cinovec, Podlesí, Sejby and Honolka granites (Czech Republic); Chavance and Les Châtelliers granites (France); Beauvoir, Montebbras granites and Richemont rhyolitic dike (France); Argemela (Portugal)
III	Peraluminous	Ta, Sn, Li, F	continental-collision	0.1 % to 0.57 %	0.21 % to 1.22 %	Lepidolite, Li-rich muscovite and amblygonite	

feldspar, micas, with various amounts of garnet, tourmaline, apatite and (usually) accessory Li-bearing minerals – locally rock-forming – such as spodumene, petalite, etc. Although not systematically observed, LCT pegmatites generally show layering and/or concentric zoning. Lithium-bearing minerals, including spodumene, petalite, the amblygonite-montebrasite group, lepidolite (Fig. 2D, E), eucryptite, elbaite and the lithiophilite-triphylite group are commonly found in pegmatite bodies, whereas cookeite and holmquistite occur mainly in the pegmatite aureole, or as secondary minerals (e.g., cookeite after petalite). Note that eucryptite may reflect the alteration of primary spodumene. Li₂O content varies as a function of the LCT pegmatite subtype and the Li-bearing minerals themselves (Table 3), ranging from 0.5 to 1.5%.

Mixed niobium–yttrium–fluorine (NYF)-LCT pegmatites are known from Norway (e.g., Birkeland, Frikstad, Skripeland) and Ukraine (Volodarsk-Volynsky). In Norway, pegmatite fields such as Evje-Iveland show a typical initial NYF chemical signature, but are depleted in REEs and F in replacement areas. Moreover, the replacement zones show a “cleavelandite signature” as well as chemical and mineralogical LCT features, including beryl, columbite group minerals and tourmaline (Černý, 1991a,b). Lithium-ore tonnages or grades are not reported for these pegmatites.

2.1.3. Greisen

Greisen deposits (e.g., St Austell, UK; Cinovec, CZ) result from a high-temperature hydrothermal transformation of fractionated granitic intrusions (pegmatites, granites) with their upper part being a porous muscovite-quartz assemblage at the granite/host-rock contact. They can occur as multi-stage swarms crosscutting Sn-W quartz veins (e.g., Černý and Ercit, 2005; Štemprok et al., 2005; Launay et al., 2019), or may form up to 100-m thick units with irregular to sheet-like bodies. Li is mainly hosted in micas, such as Li-rich muscovite, lepidolite, zinnwaldite, and amblygonite-montebrasite group minerals. Peraluminous RMG and metaluminous intrusions are favorable rock types for the development of such deposit types (Fig. 1C), whereas fractionated granites appear to be unrelated with significant Li endowment. Thus, the Li₂O content in the greisen around the world-class Panasqueira W deposit (Portugal) is only about 732 ppm (Bussink, 1984), whereas Li₂O values from the Erzgebirge province (e.g., Štemprok et al., 2005; Jarchovský, 2006) vary from 80 to 3100 ppm for greisen of the RMG Vykmánov and Schnöd granites.

Quartz, cassiterite, wolframite, micas, topaz, tourmaline, sericite and chlorite are common in greisen, showing vertical and horizontal zoning. Alteration is generally shown by kaolinization, tourmalinization, feldspathization (microclinization and/or albitionization) and greisenization forming haloes around the granitic body. REE enrichment may occur and is indicated by precipitation of monazite, xenotime and other REE-rich minerals.

Note that this deposit type can be related to both magmatic and hydrothermal processes. Here, we consider a “granite-related” classification even though hot hydrothermal fluids are involved.

Co-products commonly consist of industrial minerals, such as feldspar, quartz and kaolin (e.g., Beauvoir, France); Sn and W are of first interest, Be, Ta, In, Sc, Rb representing potential byproducts.

2.1.4. Quartz-montebrasite hydrothermal veins

Several authors (e.g., Martín-Izard et al., 1992; Roda-Robles et al., 2016) reported the existence of quartz-montebrasite hydrothermal veins associated with leucogranitic cupolas in the central part of the Central Iberian Zone in Spain (e.g., Valdeflores, Barquilla, Golpejas, El Trasquillo) and Portugal (e.g., Argemela area and Massueime).

Hosted by granites or metasedimentary rock of the Schist-Metagreywacke Complex, these veins are generally < 1 m thick and fill fracture sets. They contain a high proportion of quartz and few minerals such as K-feldspars and micas (Roda-Robles et al., 2016). Accessory minerals such as Nb-Ta oxides, cassiterite and sulfides are common, and Li-bearing minerals consist of the montebrasite-amblygonite series (Table 1). Note that only few Li₂O values are reported for these occurrences (i.e.,

Table 3

Pegmatite classification according to Černý and Ercit (2005) and Černý et al. (2012) and corresponding P/T conditions. (See above-mentioned references for further information.)

Class	Subclass	Type	Subtype	Host rock Temp	Pressure	Family	Examples	References
Abyssal	HREE					NYF		
	LREE			700–800 °C	> 5 kbar	NYF		
	U					LCT		
Muscovite	B/Be			650–580 °C	5 to 8 kbar			
Muscovite-rare element	REE			650–520 °C	3–7 kbar	NYF		
	Li					LCT		
Rare element	REE	allanite-monazite euxenite gadolinite		variable	variable	NYF		
		beryl	beryl-columbite beryl-columbite-phosphate				Moravany, Slovakia Pedra da Moura, Portugal	Uher et al., 2010 Roda-Robles et al., 2016
			spodumene				Aljó, Portugal	Lima, 2000
	Li	complex	petalite lepidolite elbaite amblygonite	650–450 °C	2–4 kbar	LCT	Varutrask, Sweden Rozná, Czech Republic Ctidružice, Czech Republic Viitaniemi, Finland	Černý and Ercit, 2005 Melleton et al., 2012 Novák and Povondra, 1995, Lahti, 1981
		albite-spodumene albite					Most of the Barroso-Alvão, Portugal	Lima, 2000
Mariolitic	REE	topaz-beryl gadolinite-fergusonite		low P		NYF		
	Li	beryl-topaz spodumene petalite lepidolite		500–400 °C	3–1.5 kbar	LCT	Gwernavalou, France	Marcoux, 2018

0.45% Li₂O on average for the Argemela mine, PANNN, 2017) and, except for the Argemela mine, such deposits appear to be relatively uneconomic in view of their small size.

2.1.5. Tosudite mineralization related to gold deposits

An occurrence of Li-bearing tosudite in the Châtelet gold deposit (France) was reported in several studies (Braux et al., 1993; Piantone et al., 1994); Li₂O values range from 142 to 920 ppm. These authors suggested that the Li is related to late hydrothermal fluid circulation, itself related to the RMG emplacement in the northern part of the French Massif Central.

2.2. Sedimentary/hydrothermal/supergene deposits

These types include deposits related to either sedimentary rocks affected (or not) by hydrothermal processes, or surficial rocks affected by supergene weathering.

2.2.1. Jadar deposit type

In 2004, Rio Sava (a subsidiary of the Rio Tinto mining corporation) discovered the Jadar Basin in Serbia, now considered as a “non-conventional” world-class lithium deposit through the occurrence of the mineral jadarite (Stanley et al., 2007), a lithium boron silicate (Table 1). The basin consists of a relatively large (> 20 km long) intramontane lacustrine (paleo)-evaporite basin composed of dolomite, marble, various siliciclastic sedimentary rocks, pyroclastic units and notable oil shales (Obradovic et al., 1997). The mineralization is hosted in a 400–500 m thick Miocene sedimentary unit dominated by calcareous claystone, siltstone, sandstone and clastic rocks, unconformably overlying a Cretaceous basement composed of various metasedimentary rocks, limestone, sandstone and granite, including Miocene intrusions (Fig. 1D).

The lithium and borate mineralization occurs as 1.5 to 35 m thick stratiform lenses of three gently dipping tabular zones covering a surface area of 3 by 2.5 km. The ore is composed of jadarite-bearing siltstone and mudstone with locally interbedded sodium borate lenses (i.e., eucryptite, kernite, borax; Fig. 1D). Jadarite occurs as 1–10 mm white and rounded grains, nodules or concretions in the siltstone or mudstone matrix that contains various amounts of calcite, dolomite, K-feldspar, rutile, albite, pyrite, muscovite and ilmenite (Fig. 2F; Rio Tinto, 2017).

Stanley et al., 2007). In 2017, the mineral resources were reported as 135.7 Mt of ore at a grade of 1.86% Li₂O and 15.4% B₂O₃ (Rio Tinto, 2017), representing a giant deposit of 2.524 Mt of Li₂O.

2.2.2. Mn-(Fe) deposits

Among the various types of host-rocks for Li-bearing minerals in Europe, the small-scale and discontinuous Mn-Fe-rich sedimentary units (e.g., Drosogol Mine in Scotland and Clews Gill in England), exploited in the 19th century for their Fe and Mn contents, are a favorable site for secondary Li-oxides such as lithiophorite (Table 1). Stratigraphically, they can be subdivided into two distinct units: 1) a reddish siliciclastic host rock, mainly pelite, shale and/or sandstone, enhanced in Mn and Fe relative to the average shale composition; and 2) discontinuous Mn lenses or layers (coticules). The minerals include cryptomelane, goethite, hematite and other manganese oxides including Li-rich lithiophorite, chalcophanite and pyrolusite.

The Li₂O content in lithiophorite is relatively low (1.23 wt% for Li₂O versus 55 wt% for MnO), indicating an uneconomic lithium grade. However, its occurrence is relatively important in view of the sedimentary and European histories (cf. Section 3 hereafter).

2.2.3. Bauxite deposits

Similar to the Mn-Fe deposit type, bauxite deposits can contain various amounts of lithiophorite, cookeite (Table 1) and tosudite (Li-rich gibbsite; Nishiyama et al., 1975). Lithiophorite is the most common Li-bearing manganese oxide mineral in karst bauxites. It occurs in several localities, such as the Halimba, Fenyöfö and Kincsesbanya deposits in Hungary, where aluminum and gallium in bauxite deposits were exploited from the 1950s to recently (Anderson, 2015).

Al and Mn are of first interest in this deposit type. The presence of lithiophorite and local cookeite reflect Li enrichment, though this is not systematically evaluated. However, values of up to 0.53% Li₂O within bauxite are known from China (Wang et al., 2013) and the USA (Tourtelot and Brenner-Tourtelot, 1977).

2.2.4. Other lithium deposit types

A few other deposit types show relatively minor anomalous lithium contents, including: 1) Mississippi-Valley type (MVT) deposits that

include some lithiophorite (Usingen, Germany), and 2) Aalenian black shales from the Dauphinois region, Isère, France, where cookeite is disseminated in black shale and in tension gashes crosscutting the shales (Jullien and Goffé, 1993). For the latter occurrence, values (Henry et al., 1996) are in the range of 9 to 1 847 ppm Li₂O with an average of 441 ppm Li₂O (n = 10). These lithium occurrences are symptomatic for local conditions allowing minor enrichment, implying that they are not economically significant regarding their Li content.

2.3. Lithium resources and reserves

In Europe, lithium resources and reserves have been estimated or evaluated according to a CRIRSCO (i.e., Committee for Mineral Reserves International Reporting Standards) reporting system, or based on historical evaluations, for only 35 sites (Table 4). Thirteen occurrences in England, Ireland, France and Germany, such as Beauvoir, Montebbras, St Austell or Aclare, were evaluated before systematic reporting was established, and their mineral-resource and -reserve estimates are mostly based on historic evaluations by geological survey organizations. Fifteen projects, including Jadar, are defined in the Australian JORC classification; one project (Zinnwald) was defined in the European PERC; one project (Alberta I) is defined in the Canadian NI43-101 system; Four projects in Ukraine are defined in an unknown system (Table 4); and one project is defined in the United Nations Framework Classification (UNFC). This list reflects the active exploration of lithium in Europe.

However, most of these deposits report mineral resources and only five specify reserve values, indicating that a feasibility study was carried out. This generally includes a study of potential processing and metallurgical-treatment methods, resulting in an economically feasible recovery of lithium from the various Li-bearing minerals.

In order to compare the Li-content in known Li-deposits, the sum of ore production + ore reserves + ore resources has been converted into contained Li₂O (ore tonnage × ore grade) for each deposit. These deposits were then categorized and classified into categories A, B, C, D and E¹ according to their commodities and their reported mineral resources and -reserves (Table 4), following the system of the European ProMine database (Cassard et al., 2015). Note that we consider only the A, B, C and D categories as (potential) lithium deposits (Table 4), which corresponds to 28 deposits.

Among them, three deposits are identified as category A, including the Cinovec (Czech Republic), St Austell (UK) greisen and the Jadar deposit (Serbia). However, the historical estimate by the British Geological Survey for the St Austell deposit may be unrealistic, as it was based on extraction from an area of about 92.5 km² on the edges of protected landscape zones (British Geological Survey, 2016).

Lithium occurrences appear to be well distributed in Europe. However, the Iberian area and Finland regroup most of the identified lithium deposits (Table 4), indicating that these countries are relatively active in lithium exploration and suggesting that they have a strong Li-potential.

3. Lithium metallogeny in Europe throughout the earth's evolution

In Europe, several orogenic events throughout geological history are associated with lithium mineralization. In this section, we assess and contextualize the lithium mineralization to orogenic features in order to establish—if possible—potential metallogenetic settings.

As a reminder, Europe's landmass results from a long geological history spanning 3.6 billion years, including the assemblage of

numerous continental blocks. The European lithosphere can be broadly divided into two large regions: 1) The old East European Craton, partly covered by weakly deformed Phanerozoic and Mesoto Neo-Proterozoic rift and platform successions, mostly located in eastern and north-eastern Europe; and 2) A thinner, dominantly Phanerozoic, lithosphere, accreted to the East European Craton during Palaeozoic and younger orogenies, mostly in Western Europe (e.g., Gee et al., 2006; Artemieva and Thybo, 2013).

3.1. Hard-rock lithium mineralization in European Archean to Paleo-Proterozoic terranes

3.1.1. The Ukrainian Shield (3.5 to 1.9 Ga)

The Ukrainian Shield forms an assembly of Precambrian crystalline megablocks that is 900 km long and 60–150 km wide in the central part of the country (Fig. 3A). This area is fault-bounded by the younger Dnister-Fore Black Sea and the Dniprovsко-Donnetska metallogenic provinces, and was affected by three distinct magmatic events at ca. 3.2, 2.6 and 1.9 Ga (Vinogradov and Tugarinov, 1961), which may have been partly coeval with the Svecofennian magmatism (2.1 to 1.8 Ga).

Several Li-rich deposits and occurrences are reported, such as: 1) the spodumene- and petalite- subtype of lithium-cesium-tantalum (LCT) pegmatites that occur in the Dnester-Bug (Podolia) and Azov Megablocks (e.g., Krutaya Balka, Nadyia); and 2) zinnwaldite and lepidolite occurrences in mixed miarolitic niobium-yttrium-fluorine (NYF)-LCT pegmatites (e.g., Volodarsk-Volynsky) and rare-metal granites (RMG), such as the Perzhanskoe ore district in the Northern Volyn Megablock (Kvasnista et al., 2016).

Although these lithium occurrences are known, only very little information is available. This makes their evaluation, regarding metallogenetic settings and geological context from a European perspective, very difficult.

3.1.2. The Svecofennian orogenic belt (2.1 to 1.8 Ga)

The Svecofennian orogenic belt (Fig. 3) is part of the Columbia/Nuna supercontinent accretion that took place from 2.1 to 1.8 Ga (Zhao et al., 2002). It consists of magmatic-arc accretionary phases joining the juvenile Svecofennian arc terrane to the Archean Karelia Craton (Nironen, 1997) along the Luleå-Kuopio thrust zone (Fig. 3; Zhao et al., 2002).

Prior to the Svecofennian orogen, continental break-up of the Karelian Province led to the formation of an ocean basin and deposition of sedimentary units such as the 1.92 Ga Pohjanmaa schist belt. Initial accretion started at 1.91 Ga and ended at 1.87 Ga, followed by large-scale extension in a back-arc setting (1.87–1.84 Ga) shown by psammites/pelites and intruded by granites and mafic dikes (Korja et al., 2006). An oblique continent-continent collision occurred from 1.87 to 1.79 Ga, illustrated by the advancing accretion of retro-arc fold-and-thrust belts with alkaline bimodal magmatism (e.g., Lahtinen et al., 2009). Significant lithospheric thickening, local migmatization and formation of S-type granites in southern Finland and central Sweden occurred as well. Finally, gravitational collapse ended the orogen between 1.79 and 1.77 Ga. Two major amphibolite grade metamorphic events are recorded at 1.88–1.87 Ga (Lecomte et al., 2014) and 1.83 to 1.80 Ga (Eilu et al., 2012).

Within this geological framework, lithium mineralization took place in metasedimentary and metavolcanic units along major fault and shear zones. They are dated as relatively late, between 1.8 and 1.79 Ga (Fig. 3, Table 5; e.g., Alviola et al., 2001), post-dating local migmatization. They include the ca. 1.88–1.86 Ga Vaasa Migmatite Complex on the margins of the Evijärvi belt (Suikkanen et al., 2014), and the ca. 1.84–1.82 Ga late-orogenic migmatizing microcline granites in south-western Finland (Kurhila et al., 2005), and appear coeval with the regional amphibolite-grade metamorphism. The mineralization occurs as LCT pegmatite fields, such as the Kaustinen and Somero-Tammela fields (Fig. 3). The Kaustinen one occurs in the 1.92 Ga Pohjanmaa schist belt comprising the Länttä, Syväjärvi and Outovesi deposits, which are albite-spodumene pegmatites owned by Keliber Oy. In the Somero-Tammela region (Fig. 3), the petalite/spodumene Luolamaki,

¹ Category refers to: Category A ≥ 1,000,000 t Li₂O; 1,000,000 t ≥ Category B ≥ 100,000 t Li₂O; 100,000 t ≥ Category C ≥ 50,000 t Li₂O; 50,000 t ≥ Category D ≥ 5,000 t Li₂O; Category E < 5,000 t Li₂O, based on the sum of production + reserves + resources.

Table 4
Li projects in Europe and their past production and estimated Li metal resources/reserves. NA refers to data not available. (data were collected from mining companies; Lulzac and Apolinarski, 1986; Smolin and Beaudry, 2015; British Geological Survey, 2016).

Prospect	Project	Country	Company	Past Production Li ₂ O (t)	Past Production Li metal (t)	Grade past-prod. Li ₂ O (%)	Resource Tonnage (t)	Resources Li ₂ O (t)	Resources Li metal (t)	
Cinovec	Cinovec	Czech Republic	European Metals	NA	NA	69,59,00,000,00	29,21,631,77	13,55,637		
St Austell	St Austell	England	Rio Tinto	NA	NA	26666666700,00	1,60,00,000,02	74,24,000		
Jadar	Jadar	Serbia	NA	–	–	13,57,00,000,00	25,24,020,00	11,71,45		
Nadiya	Nadiya	Ukraine	NA	NA	NA	6,50,80,000,00	7,28,896,00	3,38,208		
Vaidelíórez/San José	Valdeñórez/San José	Spain	Infinity Lithium Corporation Ltd/ Valoriza Minería S.A.	–	–	11,20,00,000,00	6,83,200,00	3,17,005		
Stankovaskoe	Stankovaskoe	Ukraine	NA	NA	NA	3,61,53,800,00	4,69,999,40	2,18,080		
Beauvoir	Beauvoir	France	Imerys	NA	NA	4,30,00,000,00	3,05,300,00	1,41,659		
Mina do Barroso	Mina do Barroso	Portugal	Savannah Resources Plc /Slipstream Grandao, NOA	–	–	2,35,00,000,00	2,41,000,00	1,11,833		
Zinnwald	Zinnwald	Germany	Bacanora Minerals Ltd/ SolarWorld	–	–	3,55,10,000,00	1,24,959,69	57,981		
Sadisdorf	Sadisdorf	Germany	Lithium Australia	NA	NA	2,50,00,000,00	1,12,500,00	52,200		
Wolfsberg	Wolfsberg	Austria	European Lithium	NA	NA	1,09,80,000,00	1,09,800,00	50,947		
Romano/Sepeda	Romano/Sepeda	Portugal	Novo Lítio/Lusorecursos	–	–	1,03,00,000,00	1,03,000,00	47,792		
Altenberg	Altenberg	Germany	Ukrainian rare metals	1,99,124,75	92,500	0,185	NA	NA		
Polojohovskoe	Polojohovskoe	Ukraine	Ukrainian rare metals	–	NA	61,33,000,00	88,928,50	41,263		
Shevchenkovskoe	Shevchenkovskoe	Ukraine	NA	NA	NA	63,60,000,00	69,960,00	32,461		
Tréguennec - Prat-ar-Hastel	Tréguennec - Prat-ar-Hastel	France	–	NA	NA	85,00,000,00	66,300,00	30,763		
Alberta I	Alberta I	Spain	MineworX	–	–	1,74,00,000,00	66,120,00	30,680		
Alvarrões	Alvarrões	Portugal	Lepidico Ltd/Felmica	–	–	58,70,000,00	51,069,00	23,698		
Rapasaari	Rapasaari	Finland	Keliber Oy	–	–	44,29,000,00	50,047,70	23,222		
Argemela	Argemela	Portugal	NA	NA	NA	1,11,00,000,00	49,950,00	23,178		
Meldon aplite quarry	Meldon aplite quarry	England	NA	NA	NA	1,33,82,400,00	45,500,16	21,112		
Syyäjärvi	Syyäjärvi	Finland	Keliber Oy	–	–	26,908,00	12,485	12,485		
Länttiä	Länttiä	Finland	Keliber Oy	–	–	13,30,000,00	13,832,00	6,418		
Emmes	Emmes	Finland	Keliber Oy	–	–	10,80,000,00	13,176,00	6,114		
Aclare	Aclare	Ireland	International Lithium	–	–	5,70,000,00	8,550,00	3,967		
Montebras	Montebras	France	Imerys	4,305,40	2,000	–	3,66,700,00	5,50,50	2,552	
Alijo	Alijo	Portugal	José Aldeia Lagoa & Filhos, SA	15,236,81	7,078	NA	4,02,800,00	5,639,20	2,617	
Ghéderville	Ghéderville	France	Keliber Oy	–	–	3,00,000,00	3,00,000,00	1,392		
Leviäkangas	Leviäkangas	Finland	Scandanian Metals/Nortec Minerals Corp	–	–	4,90,000,00	4,865,70	2,258		
Kietynmäki	Kietynmäki	Finland	Keliber Oy	–	–	4,00,000,00	4,720,00			
Outovesi	Outovesi	Finland	Scandanian Metals/Nortec Minerals Corp	–	–	2,80,000,00	4,004,00	1,858		
Hirvikallio	Hirvikallio	Finland	–	–	–	1,50,000,00	2,685,00			
Tréguennec - Tréluan	Tréguennec - Tréluan	France	–	–	–	34,12,921,35	1,215,00	564		
Cornelia Mine	Cornelia Mine	Germany	–	297,07	138	8,6	NA	NA		
Silbergrube	Silbergrube	Germany	–	2,152,70	1,000	NA	NA	NA		
							Total resources	89,06,278		

(continued on next page)

Table 4 (continued)

Prospect	Grade resources Li ₂ O (%)	Category re-sources	Reserves Tonnage (t)	Reserves Li ₂ O (t)	Reserves Li metal (t)	Grade reserves Li ₂ O (%)	Category reserves	Code	Status
Cinovec	0.419835%	A	—	—	—	—	—	JORC	Prospect under (downstream) evaluation
St Austell	0.06%	A	—	—	—	—	—	Historical Estimate	Producing deposit
Jadar	1.86%	A	—	—	—	—	—	JORC	Deposit under development - project
Nadiya	1.12%	B	—	—	—	—	—	Unknown	Deposit or prospect of unknown status
Vaideñorrez/San José	0.61%	B	—	—	—	—	—	JORC	Deposit under development - project
Stankovasroe	1.3%	B	—	—	—	—	—	Unknown	Deposit or prospect of unknown status
Beauvoir	0.71%	B	—	—	—	—	—	Historical Estimate	Producing deposit
Mina do Barroso	1.02%	B	—	—	—	—	—	JORC	Deposit under development - project
Zinnwald	0.3519%	B	—	—	—	—	—	PERC	Prospect under (downstream) evaluation
Sadisdorf	0.45%	B	—	—	—	—	—	JORC	Prospect under (downstream) evaluation
Wolfsberg	1.00%	B	—	—	—	—	—	JORC	Prospect under (downstream) evaluation
Romano/Sepeda	1.00%	B	—	—	—	—	—	Deposit under development - project	Deposit under development - project
Altenberg	NA	C	—	—	—	—	—	Deposit or prospect of unknown status	Deposit or prospect of upstream reconnaissance
Polokhovskoe	1.45%	C	—	—	—	—	—	Unknown	Prospect under (upstream) reconnaissance
Shevchenkovskoe	1.1%	C	—	—	—	—	—	Unknown	Deposit under development - project
Tréguennec - Prat-ar-Hastel	0.78%	C	—	—	—	—	—	Historical Estimate	Unexploited deposit
Alberta 1	0.38%	C	—	—	—	—	—	NI 43-101	Deposit under development - project
Alvarrões	0.87%	C	34,90,000.00	38,041.00	17,651	—	—	JORC	Deposit under development - project
Rapassari	1.13%	C	—	—	—	—	—	JORC	Prospect under (downstream) evaluation
Argamela	0.21%	D	—	—	—	—	—	JORC	Prospect under (downstream) evaluation
Meldon aplite quarry	0.34%	D	17,55,000.00	20,709.00	9,609	—	—	Historical Estimate	Prospect under (downstream) evaluation
Svärjärv	1.24%	D	10,77,000.00	9,262.20	4,298	—	—	JORC	Prospect under (downstream) evaluation
Läntä	1.04%	D	8,63,000.00	8,716.30	4,044,3632	1.01%	—	JORC	Prospect under (downstream) evaluation
Emmes	1.22%	D	—	—	—	—	—	Historical Estimate	Prospect under (downstream) evaluation
Aclare	1.5%	D	—	—	—	—	—	Historical Estimate	Prospect under (downstream) evaluation
Montebras	1.5%	D	—	—	—	—	—	Code UNFC	Producing deposit
Alijo	1.4%	D	—	—	—	—	—	Historical Estimate	Producing deposit
Chéderville	1.00%	D	—	—	—	—	—	JORC	Unexploited deposit
Leviakangas	0.993%	E	—	—	—	—	—	Historical Estimate	Deposit or prospect of unknown status
Kiectönniki	1.18%	E	—	—	—	—	—	JORC	Deposit under development - project
Outovesi	1.43%	E	2,22,000.00	2,397.60	1,112	—	—	Historical Estimate	Deposit under development - project
Hirvikallio	1.79%	E	—	—	—	—	—	Prospect	Prospect
Tréguennec - Tréuan	0.0356%	E	—	—	—	—	—	Historical Estimate	Mineral occurrence
Cornelia Mine	NA	E	—	—	—	—	—	Historical Estimate	Mineral occurrence
Silbergrube	NA	E	—	—	—	—	—	Historical Estimate	Mineral occurrence

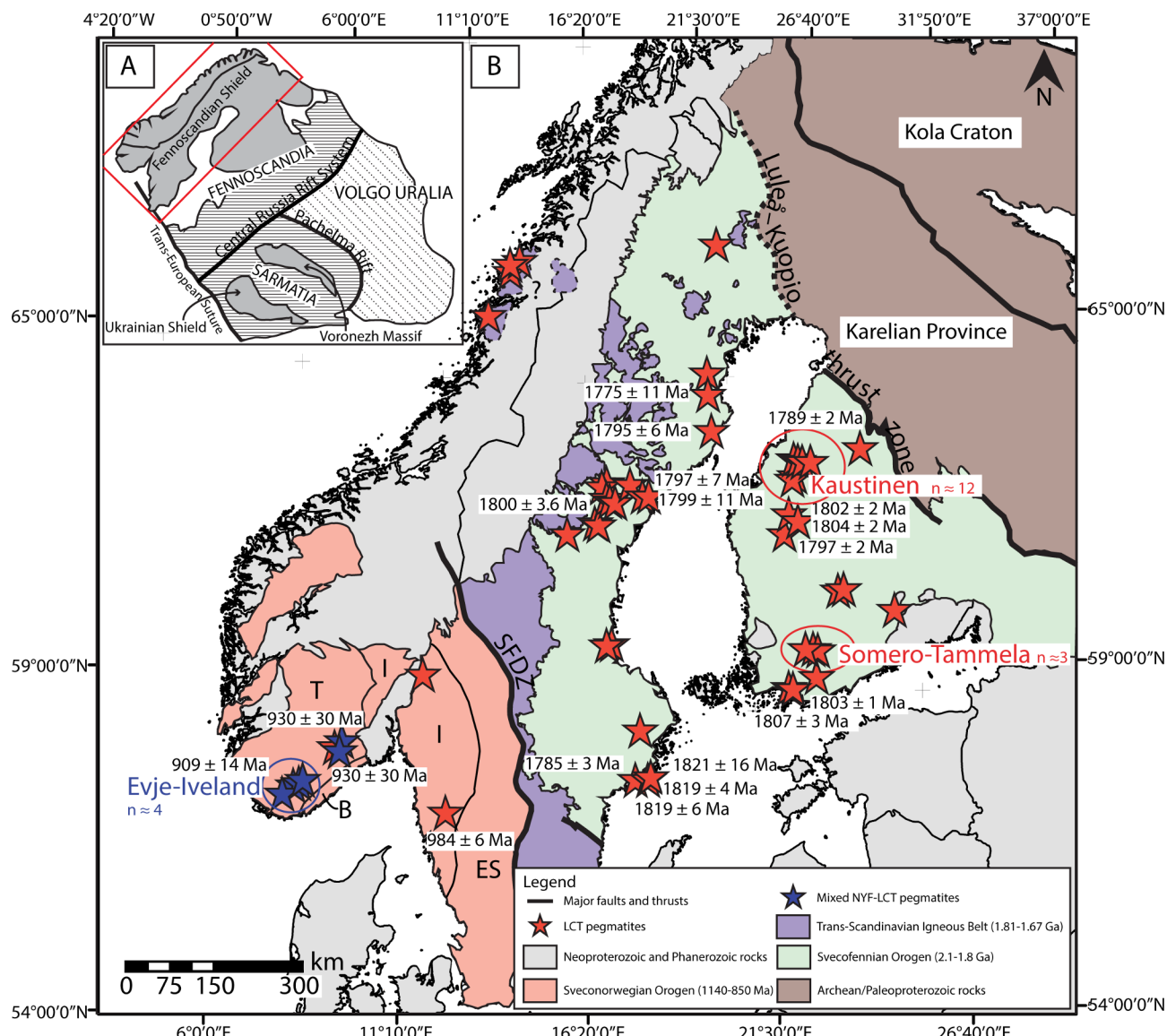


Fig. 3. A) Schematic map of the East European Craton and distribution of the main shields (modified after Roberts and Slagstad, 2015). The red box highlights the studied area. B) Simplified geological map of the Fennoscandian Shield (modified after Koistinen et al., 2001; Bergh et al., 2015) showing distribution of the Svecofennian and the Sveconorwegian orogens, and distribution of LCT and mixed NYF-LCT pegmatites. Red circles and surrounded red names refer to LCT pegmatite fields; blue circle and name refer to mixed NYF-LCT pegmatite field; n = number of identified pegmatite bodies. Abbreviations: B: Bamble Terrane; ES: Eastern Segment; I: Idefjorden Terrane; T: Telemark Terrane; SFDZ: Sveconorwegian Frontal Deformation Zone. (For interpretation of the references to color in this figure legend, the reader is referred to the web version of this article.)

Hirvikallio and Kietömaäki LCT pegmatites, owned by Nortec Minerals Corp., are hosted in the Håme belt that consists of metavolcanic rock intercalated with metagreywacke and metapelitic. In these pegmatites, petalite was formed first and later converted to spodumene, suggesting a temperature decrease at constant pressure during crystallization that involved rapid cooling of the terranes (Eilu et al., 2012). Triphylite is reported from several LCT pegmatites, mainly in Sweden.

3.1.3. The Sveconorwegian orogenic belt (1140 to 850 Ma)

Part of the Grenvillian orogeny, the Sveconorwegian orogenic belt is related to the collision between Fennoscandia and an undetermined major plate (likely Amazonia), which contributed to the Rodinia supercontinent assembly (e.g., Li et al., 2008). The orogen spans from 1140 to 850 Ma, amalgamating Mesoproterozoic (1750–1500 Ma) lithotectonic units separated by major shear zones (Bingen et al., 2008a,b); according to these authors, the orogen can be divided into several tectonic phases. Among these, the Arendal phase (1140–1080 Ma) marks the collision between the

Idefjorden and Telemarkia terranes (Fig. 3). This initial phase was related to closure of an oceanic basin, and subsequent accretion of a volcanic arc and a high-grade metamorphic event ($ca.$ 1140–1125 Ma). The Adger phase (1050–980 Ma) corresponded to oblique continent–continent collision, and underthrusting and burial/exhumation of the Idefjorden Terrane (Fig. 3). This phase was contemporaneous with crustal thickening of the Telemarkia Terrane, when widespread *syn-collisional* magmatism was followed by high-grade metamorphism. Finally, the Dalane phase (970–900 Ma) corresponded to gravitational collapse, associated with post-collisional magmatism, and formation of a gneiss dome and core complex (930–920 Ma) with low-pressure/high-temperature metamorphism.

In this context, lithium mineralization occurred within poly-metamorphic Paleoproterozoic amphibolite gneiss, gabbroic amphibolite and metadiorite, mainly within the Idefjorden and Telemark terranes. In the latter, the Evje-Iveland pegmatite field, recognized as the largest one (Fig. 3; e.g., Birkeland and Frikstad), comprises over 400 pegmatite bodies. These were dated at $ca.$ 909 ± 14 Ma (Scherer et al., 2001; Table 5),

Table 5
Location and dating of several pegmatite, RMG and greisen deposits in Europe.

Country	Occurrence Name	Latitude (decimal degrees)	Longitude (decimal degrees)	Orogeny	Lithology	Area	Age 1	Age 2	Mineral analyzed	Method	Reference
Sweden	Uti gruvor	59.667133	14.316415	Svecofennian	LCT pegmatite		1821	16	columbite-tantalite	U/Pb	Romer and Smeds, 1994
Sweden	Ränö	58.928539	18.180919	Svecofennian	LCT pegmatite		1819	4	columbite-tantalite	U/Pb	Romer and Smeds, 1994
Sweden	Norrö	58.885833333333	18.134444444444	Svecofennian	LCT pegmatite		1819	6	columbite-tantalite	U/Pb	Romer and Smeds, 1994
Finland	Rosendal	60.123	22.553	Svecofennian	LCT pegmatite		1807	3	ferrotapiolite	U/Pb	Lindroos et al., 1996
Finland	Kaatiala	62.679166666667	23.490555555556	Svecofennian	LCT pegmatite		1804	2	columbite-tantalite	U/Pb	Alviola et al., 2001
Finland	Skogsböle	60.142	22.598	Svecofennian	LCT pegmatite	Kemiö pegmatite field	1803	1.3	ferrotapiolite	U/Pb	Lindroos et al., 1996
Finland	Seinäjoki	62.779	23.1846	Svecofennian	LCT pegmatite		1802	2	ferrotapiolite	U/Pb	Alviola et al., 2001
Sweden	Jatkvisle	62.838055555556	16.638888888889	Svecofennian	LCT pegmatite		1800	3.6	columbite-tantalite	U/Pb	Romer and Smeds, 1997
Sweden	Dygsetet	63.24422	18.156294	Svecofennian	LCT pegmatite		1799	11	columbite-tantalite	U/Pb	Romer and Smeds, 1994
Finland	Haapaluoma	62.508	22.983	Svecofennian	LCT pegmatite		1797	2	columbite-tantalite	U/Pb	Alviola et al., 2001
Sweden	Stenbäckberget	63.239526	18.224771	Svecofennian	LCT pegmatite		1797	7	columbite-tantalite	U/Pb	Romer and Smeds, 1994
Sweden	Orrvik	64.2	20.768888888889	Svecofennian	LCT pegmatite		1795	6	columbite-tantalite	U/Pb	Romer and Smeds, 1994
Finland	Rapasaari	63.39162	23.50256	Svecofennian	LCT pegmatite	Kaustinen Li-pegmatite field	1790	NA	columbite-tantalite	U/Pb	Kuusela et al., 2011
Finland	Länttä/Ullava	63.62095997	24.14255624	Svecofennian	LCT pegmatite	Kaustinen Li-pegmatite field	1789	2	columbite-tantalite	U/Pb	Alviola et al., 2001
Sweden	Stora Vika	58.916944444444	17.815	Svecofennian	LCT pegmatite	Sörmland	1785	3	columbite-tantalite	U/Pb	Romer and Smeds, 1997
Sweden	Varutrisk	64.800555555555	20.740833333333	Svecofennian	LCT pegmatite		1775	11	columbite-tantalite	U/Pb	Romer and Wright, 1992
Sweden	Skuleboda	58.336666666667	12.116527777778	Sveconorwegian	LCT pegmatite	Idefjorden Terrane	984	6	columbite-tantalite	U/Pb	Romer and Smeds, 1994
Norway	Høydal	59.183142	8.759742	Sveconorwegian	Mixed LCT-NYF pegmatite	Idefjorden Terrane	930	30	lepidolite	K/Ar	Kulp et al., 1963 – indirect age determination
Norway	Heftejtem	59.143055555556	8.75666666666667	Sveconorwegian	Mixed LCT-NYF pegmatite	Telemark Terrane	930	30	lepidolite	K/Ar	Kulp et al., 1963 – indirect age determination
Norway	Friksstad	58.525013	7.8986257	Sveconorwegian	Mixed LCT-NYF pegmatite	Evie-Iveland pegmatite field	909	14	gadolinite	U/Pb	Scherer et al., 2001
Norway	Birkeland	58.530833333333	7.9238888888889	Sveconorwegian	Mixed LCT-NYF pegmatite	Evie-Iveland pegmatite field	909	14	gadolinite	U/Pb	Scherer et al., 2001
Ireland	Moylisha	52.747771	-6.61769	Caledonian	LCT pegmatite	Leinster pegmatite field	416.1	4.1	muscovite, K-feldspar	Rb/Sr	Barros, 2017
Ireland	Aclare	52.661918	-6.74892	Caledonian	LCT pegmatite	Sowie Gory Block	370	2.4	muscovite, K-feldspar	Rb/Sr	Barros, 2017
Poland	Michałkowa	50.7275	16.448611111111	Variscan	LCT pegmatite		339	4	muscovite feldspar/garnet	Rb/Sr	Van Breemen et al., 1988
Austria	Tannenfeld	48.439444444444	15.409166666667	Variscan	LCT pegmatite	Písek pegmatite field	339	4	monazite	Rb/Sr	Frit et al., 2012
Czech Republic	U obrazku	49.281111111111	14.276666666667	Variscan	LCT pegmatite	Jihlava pegmatite field	336	3	columbite-tantalite	U/Pb	Novák et al., 1998
Czech Republic	Pucklice	49.35035	15.679192	Variscan	LCT pegmatite	Jihlava pegmatite field	334	6	columbite-tantalite	U/Pb	Melleton et al., 2012
Czech Republic	Sedlatice	49.200453	15.612342	Variscan	LCT pegmatite	Jihlava pegmatite field					Melleton et al., 2012

(continued on next page)

Table 5 (continued)

Country	Occurrence Name	Latitude (decimal degrees)	Longitude (decimal degrees)	Orogeny	Lithology	Area	Age 1		Mineral analyzed	Method	Reference
							Age (Ma)	± 2σ			
Czech Republic	Jeclov	49.37995	15.671982	Variscan	LCT pegmatite	Jihlava pegmatite field	333	7	columbite-tantalite feldspar/garnet columbite-tantalite	U/Pb	Melleton et al., 2012
Austria	Königsalm	48.47215	15.51908	Variscan	LCT pegmatite	Strážek pegmatite field	332	3	Sm/Nd U/Pb	Ertl et al., 2012	
Czech Republic	Rožná	49.479955	16.242045	Variscan	LCT pegmatite	Strážek pegmatite field	332	3	Sm/Nd U/Pb	Melleton et al., 2012	
Czech Republic	Chvalovice	49.016787	14.222588	Variscan	LCT pegmatite	South Bohemia pegmatite field	332	3	U/Pb	Melleton et al., 2012	
Czech Republic	Dobrá Voda	49.409261	16.050951	Variscan	LCT pegmatite	Strážek pegmatite field	332	3	U/Pb	Melleton et al., 2012	
Germany	Sadisdorf	50.827222222222	13.461111111111	Variscan	Greisen	Krusné Hory Mountains	326.1	3.4	U/Pb	Zhang et al., 2017	
Portugal	Argemela	40.156042	-7.602784	Variscan	Evolved rare-metal granites		326	3	U/Pb	Melleton et al., 2015	
Czech Republic	Nová Ves	48.947464	14.252017	Variscan	LCT pegmatite	South Bohemia pegmatite field	325	2	U/Pb	Melleton et al., 2012	
Czech Republic	Krášno	50.108559	12.767297	Variscan	Greisen	Krusné Hory Mountains	323.3	1.6	Re/Os	Ackerman et al., 2017	
Czech Republic	Cidružice	48.989003	15.843322	Variscan	LCT pegmatite	Vratěnín-Radkoviče pegmatite field	323	5	U/Pb	Melleton et al., 2012	
Czech Republic	Zinnwald/Cinovec	50.73	13.766666507721	Variscan	Greisen	Krusné Hory Mountains	321.5	3.1	U/Pb	Zhang et al., 2017	
Germany	Sauberg mine	50.64083	12.97833	Variscan	Greisen		320.8	2	U/Pb	Romer et al., 2007	
Czech Republic	Krupka	50.6633	13.8667	Variscan	Greisen	Krusné Hory Mountains	320.1	2.8	U/Pb	Zhang et al., 2017	
Germany	Altenberg	50.7655555555556	13.764722222222	Variscan	Greisen	Krusné Hory Mountains	319.2	2.4	U/Pb	Romer et al., 2010	
France	Tréguennec – Prat-d’Hastel	47.875073	-4.34846	Variscan	Evolved rare-metal granites		319	6	U/Pb	Gloaguen et al., 2018	
Spain	Fl-02	42.51635	-8.35222	Variscan	LCT pegmatite	Lalin-Forcarei pegmatite field	318	4.2	U/Pb	Deveaud, 2015	
France	Beauvoir	46.181308	2.953114	Variscan	Evolved rare-metal granites	Echassières	317	6	U/Pb	Melleton et al., 2015	
France	Larmont	45.98462	1.39807	Variscan	Evolved rare-metal granites		317	14	Rb/Sr	recalculated according Viallette, 1963	
France	Montebras	46.321071	2.295544	Variscan	Evolved rare-metal granites	Blond	313.4	1.4	U/Pb	Melleton et al., 2015	
France	Richemont	46.076501	1.046411	Variscan	Evolved rare-metal granites	LCT pegmatite	314	4	U/Pb	recalculated according Viallette, 1963	
Spain	Alfonsin	42.503525	-8.339867	Variscan	Evolved rare-metal granites	Lalin-Forcarei pegmatite field	312	4	U/Pb	Melleton pers. Com.	
Portugal	Lousas	41.415323	-7.799594	Variscan	LCT pegmatite	Barroso-Alvao pegmatite field	311	5	U/Pb	Melleton pers. Com.	
Portugal	AI109-02	41.622648	-7.829223	Variscan	LCT pegmatite	Barroso-Alvao pegmatite field	311	4	U/Pb	Melleton pers. Com.	
France	Chanteloube	46.0643	1.3607	Variscan	LCT pegmatite	Saint Sylvestre	311	9	Rb/Sr	recalculated according Viallette, 1963	
France	Chédeville	45.9788888888889	1.3858333333333	Variscan	LCT pegmatite		309	5	U/Pb	Melleton et al., 2015	
Portugal	Adagoi	41.60265	-7.660869	Variscan	LCT pegmatite	Barroso-Alvao pegmatite field	307	5	U/Pb	Melleton pers. Com.	
Spain	Feli open pit	41.027847	-6.8686722	Variscan	LCT pegmatite	Fregeneda-Almendra pegmatite field	307	5	U/Pb	Melleton pers. Com.	
Spain	Alberto-03	41.004381	-6.847987	Variscan	LCT pegmatite	Fregeneda-Almendra pegmatite field	307	4	U/Pb	Melleton pers. Com.	
Portugal	Bajoca Mine	40.99907	-7.01697	Variscan	LCT pegmatite	Fregeneda-Almendra pegmatite field	305	4	U/Pb	Melleton pers. Com.	
England	St Austell	50.3521	-4.83869	Variscan	Greisen		305	5	U/Pb	Neace et al., 2016	

(continued on next page)

Table 5 (continued)

Country	Occurrence Name	Latitude (decimal degrees)	Longitude (decimal degrees)	Orogeny	Lithology	Area	Age 1		Mineral analyzed	Method	Reference
							Age (Ma)	± 2σ			
Portugal	Formigoso	41.833429	-8.625814	Variscan	LCT pegmatite	Serra de Arga pegmatite field	304	9	columbite-tantalite-lepidolite	U/Pb	Melleton pers. Com.
France	Crozant	46.386782	1.626529	Variscan	LCT pegmatite		302	4	columbite-tantalite-lepidolite	Rb/Sr	recalculated according to Viallette, 1963
Portugal	Vieiros	41.321697	-7.992944	Variscan	LCT pegmatite	Seixoso-Vieiros pegmatite field	301	4	columbite-tantalite-columbite-tantalite	U/Pb	Melleton pers. Com.
Portugal	Outeiro granite	41.351054	-8.112911	Variscan	Greisen	Seixoso-Vieiros pegmatite field	301	5	columbite-tantalite-columbite-tantalite	U/Pb	Melleton pers. Com.
Portugal	Gonçalo Sul	40.435432	-7.335044	Variscan	LCT pegmatite	Gonçalo-Seixo Amarelo pegmatite field	301	3	columbite-tantalite-columbite-tantalite	U/Pb	Melleton pers. Com.
Portugal	Queiriga	40.78663	-7.738518	Variscan	LCT pegmatite	Brissago pegmatite field	300	4	columbite-tantalite-columbite-tantalite	U/Pb	Melleton pers. Com.
France	Castelau de Brassac	43.658055555556	2.49916666666667	Variscan	LCT pegmatite		300	6	lepidolite	Rb/Sr	recalculated according to Viallette, 1963
Spain	Cap de creus	42.320228	3.3175814	Variscan	LCT pegmatite		296.2	2.5	zircon	U/Pb	Van Licherveld et al., 2017
Slovakia	Surovec	48.792306	20.561275	Variscan	Evolved rare-metal granites		276	13	Monazite	U/Pb	Finger et al., 2003
Austria	Zinkenschlucht/ Lachtal	47.2638888888889	14.341944444444	Variscan	LCT pegmatite		268	2.8	whole rock/garnet	Sm/Nd	Ilickovic et al., 2017
Austria	Hohenwart	47.325	14.2416666666667	Variscan	LCT pegmatite		264	3	garnet	Sm/Nd	Ilickovic et al., 2016
Slovakia	Medvedi potok/ Hnilec	48.826263	20.488632	Variscan	Greisen		263.8	0.8	molybdenite	Re/Os	Kohút and Stein, 2004
Austria	Wildbachgraben	46.8513888888889	15.158611111111	Variscan	LCT pegmatite		261	2.5	feldspar/garnet	Sm/Nd	Thöni et al., 2008
Austria	Weinebene/ Wolfsberg	46.83405	14.99393	Variscan	LCT pegmatite		242.8	1.7	spodumene	Rb/Sr	Thöni and Miller, 2000
Switzerland	Brissago	46.1191666666667	8.71138888888889	Alpine Orogeny	LCT pegmatite	Brissago pegmatite field	24.2	2.8	zircon	U/Pb	Vignola et al., 2008

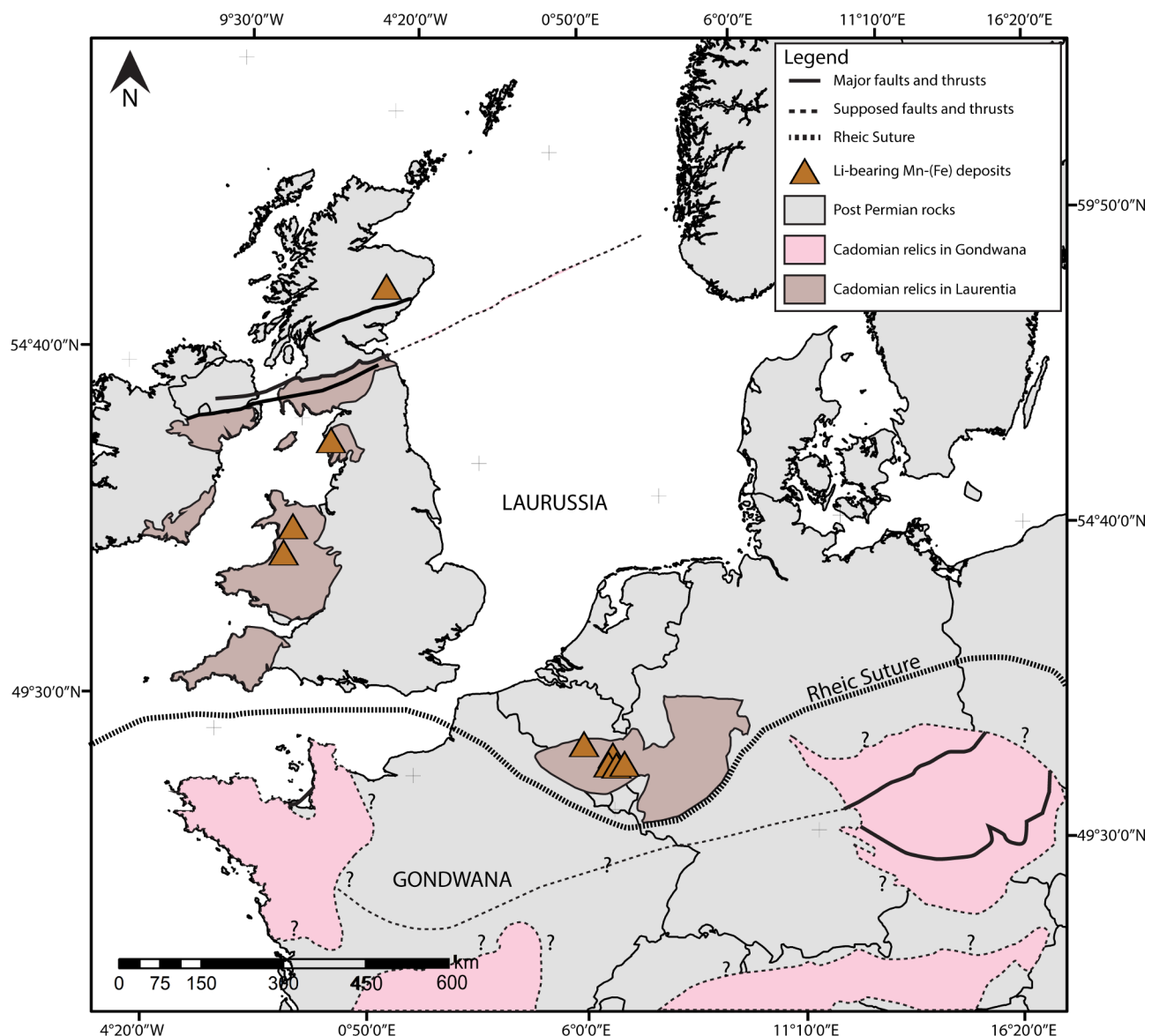


Fig. 4. Simplified geological map of the crustal block involved in the Caledonian orogeny along the Rheic Suture and location of contemporaneous Mn-(Fe) rich deposits (modified after Linnemann et al., 2007; Garfunkel, 2015). Note that Caledonian relics within Gondwana were reworked during the Variscan and Alpine orogenies making reconstruction of their respective contacts difficult.

appear to be unrelated to granites, but are coeval with late regional partial melting and crustal collapse. Among these NYF pegmatites, several indicate a late-magmatic event shown by a REE-depleted replacement zone consisting of “cleavelandite”, amazonite, quartz and muscovite, suggesting overprinting of a LCT magma onto pre-existing NYF pegmatite bodies (Černý, 1991a,b). Lepidolite and zinnwaldite are reported from these pegmatites, which are considered as mixed NYF-LCT pegmatites, although the Li enrichment is related to the replacement zones.

3.2. Hard-rock lithium mineralization in European Neoproterozoic to Neogene terranes

3.2.1. The Cadomian orogenic belt (620–540 Ma)

In Europe, the Cadomian orogeny is characterized by a continental magmatic arc, which occurred during the Ediacaran along the rim of the West African Craton and resulted in opening of the Rheic Ocean between the Avalonia and Armorica microplates, respectively associated with the Laurentia and Gondwana supercontinents. This took place from Cambrian to Ordovician (Fig. 4; e.g., Linnemann et al.,

2008; Nance et al., 2012).

A notable relic of this event is the occurrence of discontinuous Cambrian-Early Ordovician Mn-(Fe) rich metasedimentary rocks in Scotland, Wales, the Lake District of England, Belgium and Germany (Fig. 4; Kröner and Romer, 2013). Here, Li-bearing minerals such as lithiophorite can occur. Such occurrences are restricted to the Avalonian Shelf, constrained by the Rheic suture in the south, and were formed by weathering of the Cadomian continental magmatic arc at the edge of the *peri*-Gondwana plate in an extensional regime (Romer et al., 2011). They were formed during the first stage of the orogeny (ca. 590–570 Ma) and are not stratigraphically correlative, but can be found along the Avalonian Shelf from Nova Scotia through the Government Point Formation of the sedimentary Goldenville Group (Canada; White, 2008) to Poland. Kröner and Romer (2013) suggested that coeval and similar deposits may be found in the southern part of the Ossa Morena Zone (Spain).

3.2.2. The Caledonian orogenic belt (475–380 Ma)

The Caledonian orogeny was a series of tectonic events related to the closure of the Iapetus Ocean (McKerrow et al., 2000), reflecting

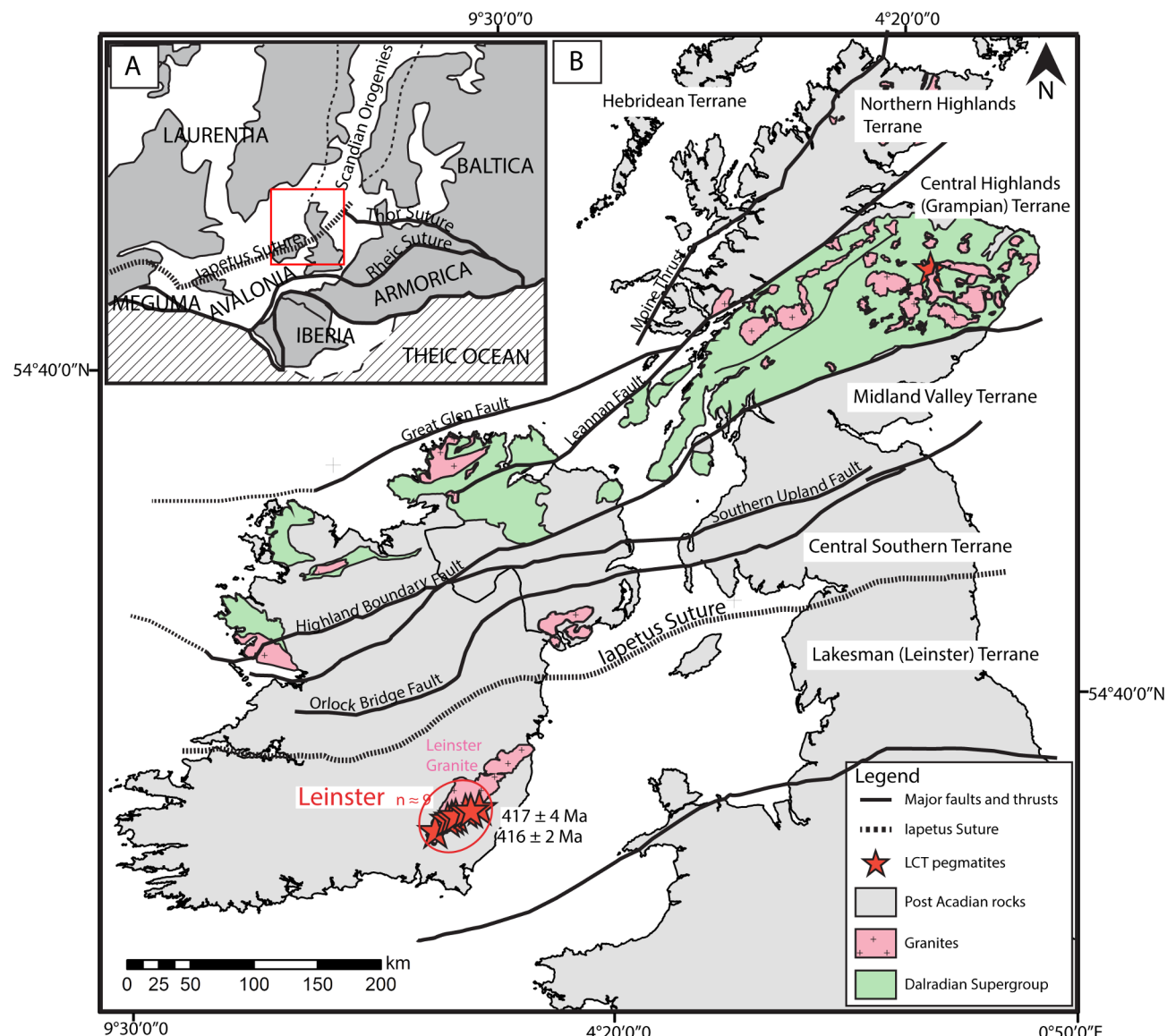


Fig. 5. A) Schematic map of the Mid-Devonian paleo-continental reconstruction (modified after Woodcock et al., 2007). Red box highlights studied area. B) Simplified geological map of Ireland and northern Britain with distribution of LCT pegmatites related to the Caledonian orogeny (modified after Miles et al., 2016). Red circle and surrounded red name refer to Leinster LCT pegmatite fields from which nine LCT pegmatites are identified. (For interpretation of the references to color in this figure legend, the reader is referred to the web version of this article.)

Ordovician-Silurian oblique interactions between the Laurentian (Scotland), Avalonia (Ireland) and Baltica terranes. The initial Grampian phase (475–460 Ma) consisted, at the north end of the Iapetus Ocean, of collision between the Laurentian continental margin and an intra-ocean island arc complex. This resulted in the emplacement of S-type granites in the NW highlands of Scotland and was followed by oblique subduction under the Laurentian (north), Avalonian (south) and Baltica (east) terranes (Fig. 5A). In the Late Silurian (425 Ma), the Iapetus Ocean was closed and continents collided with the Laurentian Terrane along the Iapetus Suture Zone (Fig. 5A). Widespread calc-alkaline magmatism occurred from ca. 425 to 380 Ma as a post-subduction event (Miles et al., 2016), related to orogen-wide sinistral transtension induced by subsequent episodes of lithospheric extension during the Early Devonian (Brown et al., 2008).

In this Caledonian context, LCT pegmatites are known from Scotland and Ireland. In Scotland, the Glenbuchat pegmatite lies in the northern part of the Iapetus Suture Zone, hosted by Dalradian metasedimentary rocks of the Grampian Terrane. It consists of lepidolite and elbaite rich pegmatite (Fig. 5B; Jackson, 1982). The Dalradian Inzie

Head gneiss and Grampian granite are associated with the ca. 470 Ma Grampian migmatization (Johnson et al., 2001).

In Ireland, the ca. 412 Ma Leinster LCT pegmatite field (Table 5; Barros, 2017) that includes the spodumene Aclare and Molyisha pegmatites, shows a relatively late time of formation (Fig. 5B). The pegmatite field is hosted by the ca. 417–405 Ma poly-phase Tullow Lowlands pluton (Fritschle, 2016) along the East Carlow Deformation Zone and includes up to 60 wt% spodumene (Luecke, 1981). Thus, their emplacement may be related to a transtensional regime in this late orogenic process.

3.2.3. The Variscan orogenic belt (400–250 Ma)

The European Variscan orogen extends from southern Iberia to northeastern Bohemia, forming a 3000 km long and 700–800 km wide belt. It results of Late Paleozoic convergence and collision of the Gondwana (south) and Laurasia-Baltica (north) megacontinents along the Variscan Front (Fig. 6), involving several intermediate microcontinents and closures of oceanic domains (e.g., Matte, 1986, 1991).

The earliest continental collision started locally in the Early Devonian (385–380 Ma) with migmatization and related anatexis of continental

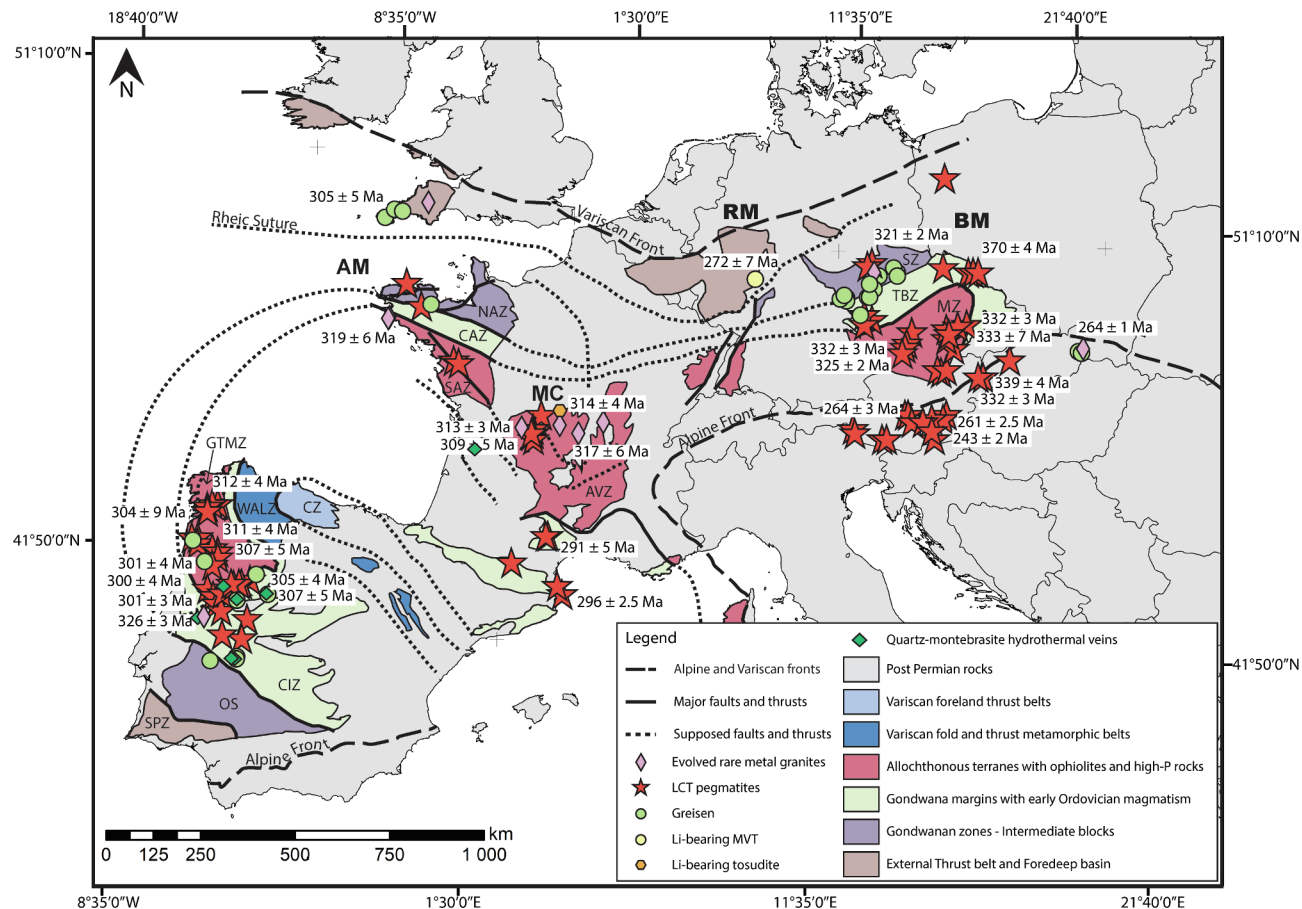


Fig. 6. Simplified geological map of the Variscan orogeny in Europe, location of various lithium-bearing deposits and a selection of ages (modified after Murphy et al., 2010; Martínez Catalán, 1990). Note that the Variscan orogeny was subsequently reworked along the Alpine Front by the Alpine orogeny. Additionally, 260 Li-rich bodies including LCT pegmatites, greisen and the Argemela RMG are identified in Portugal and Spain, 50 Li-rich occurrences are identified in the Bohemian Massif and 26 LCT pegmatites are identified in South Austria. Abbreviations: AM: Armorican Massif; AVZ: Arveno-Vosgina Zones; BM: Bohemian Massif; CAZ: Central Armorican Zone; CIZ: Central Iberian Zone; CZ: Cantabrian Zone; GTMZ: Galicia-Trás-os-Montes Zone; MZ: Moldanubian Zone; NAZ: North Armorican Zone; OS: Ossa-Morena Zone; RM: Rhenish Massif; SAZ: South Armorican Zone; SPZ: South Portuguese Zone; SZ: Saxothuringian Zone; TBZ: Teplá-Barrandian Zone; WALZ: West Asturian-Leonese Zone.

crust, as well as exhumation of Late Silurian rocks along a regional deformation event. In the Middle-Late Devonian (360–350 Ma), arc and back-arc magmatism occurred in the northern Gondwana margins and Central Armorican Domain, attesting of southward subduction and subsequent closure of the Rheic Ocean (Fig. 6; Faure et al., 2005). This event was associated with a variable pressure-temperature metamorphic and deformation event. Late Visean synorogenic extension related to a synorogenic collapse of the inner zones occurred along NW-SE stretching and 333 to 326 Ma migmatization (Faure et al., 2005). Finally, post-orogenic collapse took place around 300 Ma. It was coeval with N-S extension, development of intramontane coal basins and ca. 306 Ma local migmatization (Faure et al., 2005). These events appear to have been diachronous throughout the Variscan orogeny.

Considerable amounts of granitic intrusions and several districts of RMG/greisen and LCT pegmatite deposits illustrate the Variscan orogeny. At the scale of the belt, such deposit types are relatively late in the orogeny, coeval with crustal extension together with regional partial melting and melt emplacement. Thus, in the Bohemian Massif, the easternmost part of the European Variscan belt (Fig. 6), greisen and RMG are common in the Saxothuringian and Teplá-Barrandian zones consisting of Neoproterozoic basement (e.g., Matte, 1991). The Moldanubian area contains mainly LCT pegmatites (e.g., Cháb et al., 2010, Ackerman et al., 2017), which appear to be spatially related to migmatitic domes and shear zones. According to Melleton et al. (2012), two ages of pegmatite emplacement were identified, including an

independent orogenic stage in the Bohemian Massif with LP-HT regional metamorphism related to significant reheating and anatexis; they note that the emplacement of LCT pegmatite here is the oldest known magmatic event of the Variscan orogeny.

In France, the northwestern part of the Massif Central is a favorable area for rare-element magmatic bodies (Marignac and Cuney, 1999). This province can be divided into three distinct deposit types (Table 5): 1) rare-metal granite such as the 317 ± 6 Ma Beauvoir and the 314 ± 4 Ma Montebbras (Aubert, 1969; Cuney et al., 1992, Cuney and Alexandrov, 2002); 2) rare-metal rhyolite represented by the 313 ± 3 Ma Richemont rhyolite (Raimbault and Burnol, 1998); and 3) LCT pegmatites such as the Mont d'Ambazac rare-element pegmatite field (e.g., Raimbault et al., 1995; Deveaud et al., 2013). The latter includes the 309 ± 5 Ma lepidolite-subtype LCT Chédeville pegmatite, which postdates the 324 ± 4 Ma host granite (Hollinger et al., 1986) and appears to be sub-synchronous with local partial melting (315 ± 4 and 316 ± 4 Ma; Gébelin et al., 2009) and with shearing (La Marche shear zone: 316 ± 5 to 312 ± 2 Ma, Gébelin et al., 2007, 2009). This east-west La Marche fault system, located in the northern part of the Limousin, appears to have been a key-control on magmatic activity (Cuney et al., 2002).

The Galicia-Trás-os-Montes Zone (GTOMZ) and the Central Iberian Zone (CIZ) in the Iberian Variscan belt host widespread LCT pegmatite fields. At least five main mineralized pegmatite fields are recognized in the former from north to south: Forcarei-Lalín, Serra de Arga, Barroso-Alvão,

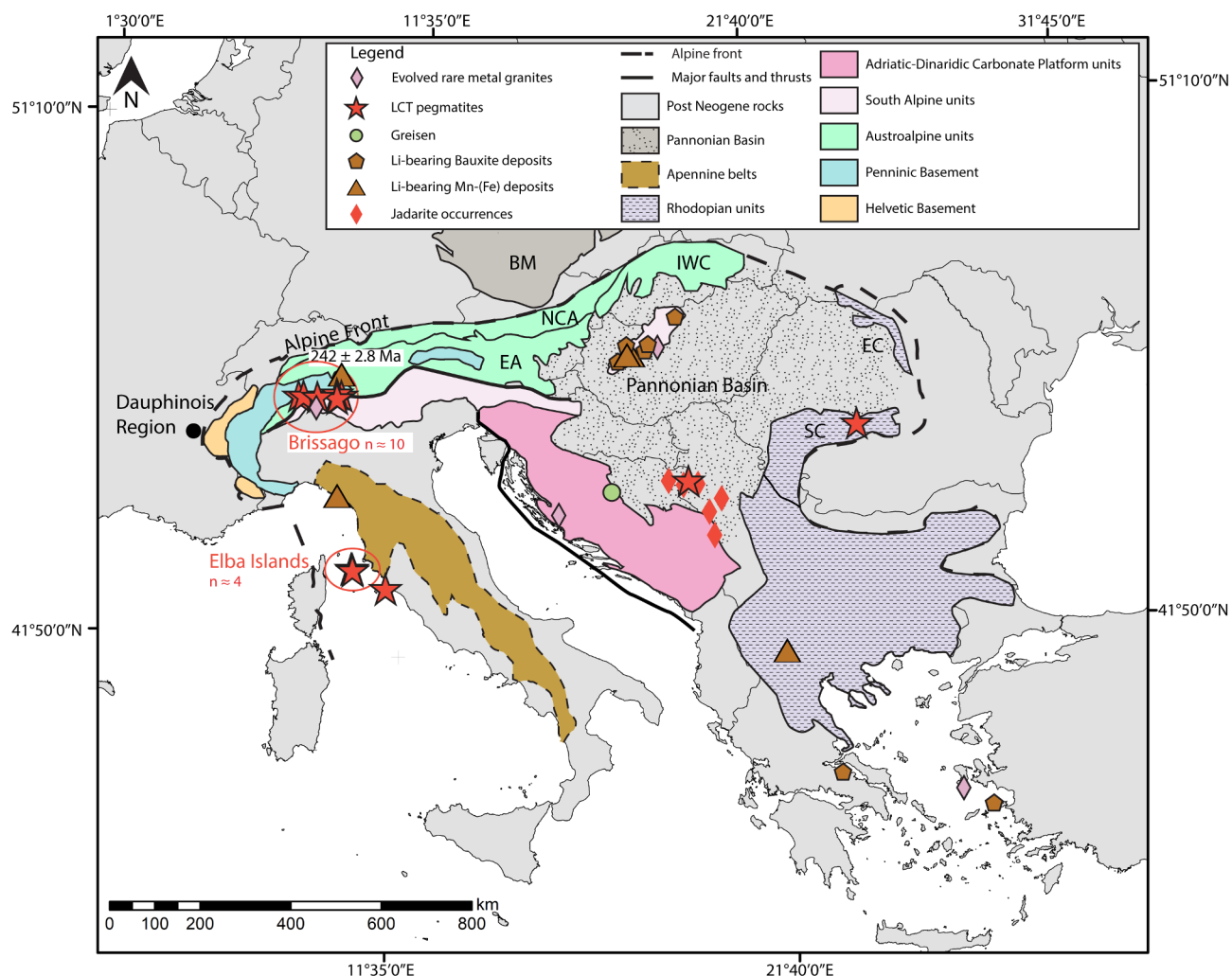


Fig. 7. Simplified geological map of the Alpine-Mediterranean area and location of lithium-bearing deposits (modified after Tomljenovic, 2002; Bousquet et al., 2012). Brissago and Elba Islands pegmatite fields are highlighted by a red circle; black circle is Dauphinois region with cookeites; n suggests number of identified pegmatite bodies. Abbreviations: BM: Bohemian Massif; EA: Eastern Alps; EC: East Carpathians; IWC: Internal West Carpathians; NCA: Northern Calcareous Alps; SC: South Carpathians. (For interpretation of the references to color in this figure legend, the reader is referred to the web version of this article.)

La Fregeneda-Almendra and Gonçalo-Guarda. In the CIZ, the 326 ± 3 Ma Argemela granite is the only RMG known from Iberia (Charoy and Noronha 1991, 1996). The average age of intrusion of LCT pegmatites in the GTOMZ is 310 ± 5 Ma, whereas in the CIZ and in the southern GTOMZ the ages are younger: 301 ± 3 Ma (Melleton et al., 2011), 295.1 ± 4.1 Ma and 296.4 ± 4.1 Ma (Roda-Robles et al., 2009; Vieira, 2010). Moreover, late quartz-montebrasite hydrothermal veins are reported from several areas in the CIZ (e.g., Roda-Robles et al., 2016).

Finally, in the Austroalpine unit of the Eastern Alps, Permian LCT spodumene-bearing pegmatites are known (e.g., Thöni and Miller, 2000; Illickovic et al., 2017). These pegmatites appear to be coeval with lithospheric extension, causing crustal basaltic underplating, HT and LP metamorphism, as well as intense magmatic activity (Schuster and Stiwe, 2008).

3.2.4. The Mediterranean and circum-Mediterranean orogens (Mesozoic-2.5 Ma)

Several styles of lithium mineralization are contemporaneous with the circum-Mediterranean and Mediterranean Tethys mountain belts, such as the Carpathians Mountains or the Egean Domain, which resulted from oceanic closure and collision of the European continental foreland (Bohemian Massif) with the African promontory of the Adriatic microplate (Fig. 7). Rifting of the Alpine Tethys and its subsequent subduction underneath the Adriatic margin, followed by continent-continent collision, promoted widespread magmatic activity

through time, as well as the development of related orogens such as the Carpathians Mountains.

The initial continental rifting of the Alpine Tethys and its related magmatism occurred from the Middle to Late Triassic in the eastern part of the Mediterranean domain (Bertotti et al., 1999; Schmid et al., 2008). In the central Alpine-Carpathian-Dinaridic orogenic system, ca. 242 Ma Li-phosphate pegmatites occur in the Brissago area (Switzerland; Vignola et al., 2008); these authors suggested that the pegmatites formed from partial melting of the Early Permian Ivrea gabbro.

This tectono-magmatic event was followed by development of the Adriatic passive margin in the Middle Jurassic (Bertotti et al., 1999; Schmid et al., 2008) in an extensional tectonic regime, and later by the subduction of the Tethys oceanic lithosphere beneath the Adriatic margin from Cretaceous to Late Paleogene. This crustal shortening led to the final consumption of the Neotethys Ocean associated with widespread calc-alkaline magmatism in the Carpathian arc (Fig. 7; Schmid et al., 2008) and formation of the Apennines in Italy. Meanwhile, Jurassic to Cretaceous bauxite deposits with lithiophorite are reported from Hungary and Greece (Fig. 7), suggesting a tropical climate during this period.

In the external domain of the Dauphinois zone (French Alps), an Eocene greenschist metamorphic event led to the formation of cookeite-bearing formations and -tension gashes within Aalenian black shales (Fig. 7). According to Jullien and Goffé (1993), the Li was sourced from the metasediments that themselves resulted from erosion of the continental crust.

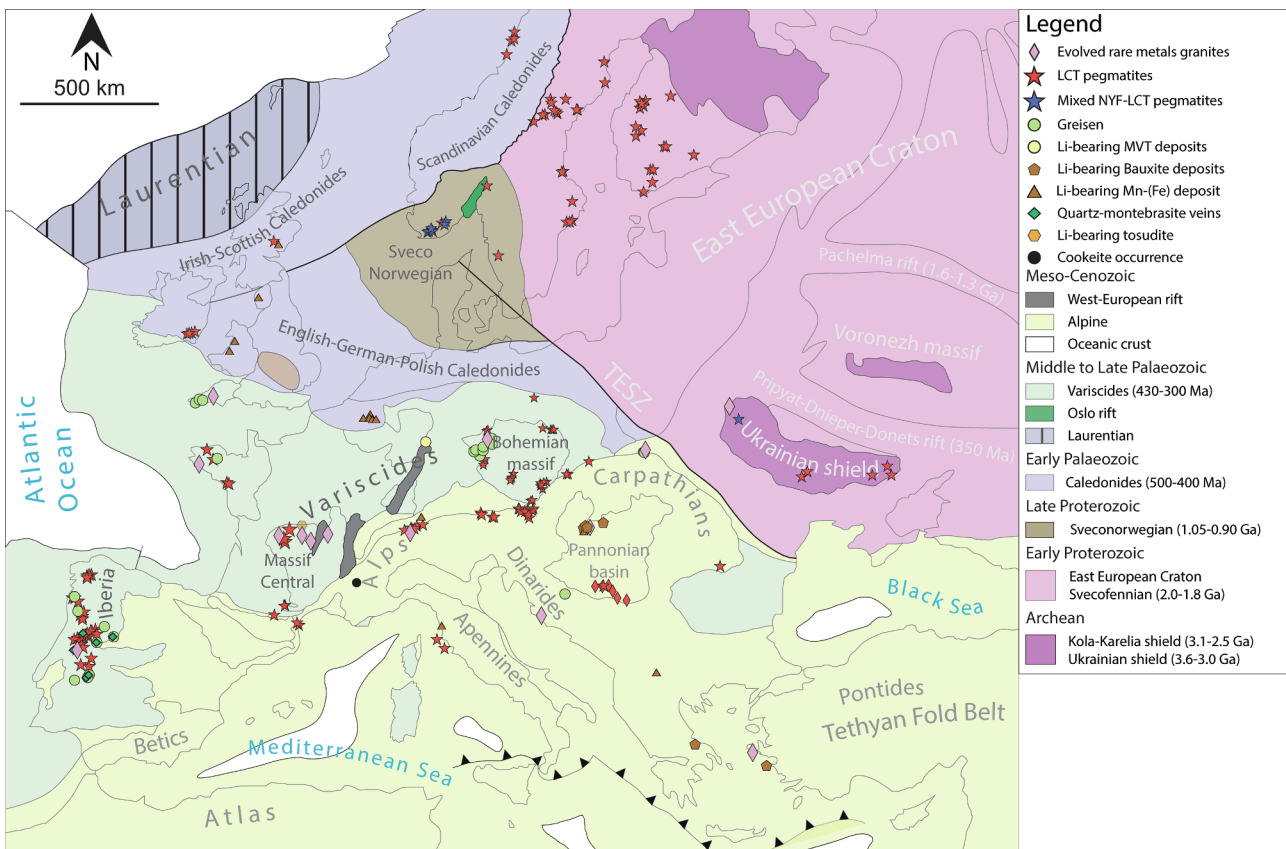


Fig. 8. Simplified geotectonic map of Europe (modified after Artemieva et al., 2006; Charles et al., 2013) and distribution of various Li-bearing occurrences.

Within the Central Alps (i.e., Penninic Zone), a kilometer-scale east-west extensional area occurs with several Oligocene-Miocene LCT pegmatites in the Vigezzo, Bodengo and Codera areas. They are Tertiary (Fig. 7; 30 to 20 Ma, Guastoni et al., 2014; Romer et al., 1996) and show a beryl-phosphate affinity with elbaite and columbite as potential accessory minerals (Guastoni et al., 2014, 2016).

Finally, extensional collapse and back-arc extension promoted development of the Miocene Pannonian and the Jadar basins within the Alpine-Carpathian-Dinarides domain along several late Oligocene–Miocene detachment zones (Jolivet et al., 2009; Menant et al., 2018; Stojadinovic et al., 2017) and in response to rapid slab roll-back (Simić et al., 2017; Stojadinovic et al., 2017). Basin formation was accompanied by calc-alkaline magmatism with a paroxysm of silicic volcanism during the early and middle Miocene (Kovács et al., 2007). Rapid exhumation of metamorphic rocks caused episodic migmatization as well as related magmatism (Bergell intrusion; Beltrando et al., 2012).

Within the northern part of the Apennines, the ca. 6.7–6.9 Ma (Ferrara and Tonarini, 1985) LCT pegmatites from Elba Island are famous for their gem-quality elbaites.

4. Interpretation and discussion

Considering all lithium occurrences in Europe, one of the first observations regarding their distribution is their apparent clustering (Figs. 3–7). This clustering defines pegmatite and/or RMG fields with similar ages of emplacement, suggesting a relatively coeval magmatic activity related to common endogenous processes. Furthermore, the Li-rich sedimentary basins such as Jadar reflect late sedimentary/hydrothermal Li re-concentration through exogenous processes.

4.1. Endogenous processes related to lithium mineralization

We have identified several Li-magmatic events through time as illustrated by RMG, greisen and LCT pegmatites (Table 5; Figs. 3–8), ranging from Paleoproterozoic to Miocene. These events occurred during times of collisional orogeny, including the Svecfennian (2.1–1.8 Ga; Fig. 3), Sveconorwegian (1140–850 Ma; Fig. 3), Caledonian (490–390 Ma; Fig. 5), Variscan (400–250 Ma; Fig. 6) and Mediterranean (Mesozoic–2.5 Ma; Fig. 7) orogenies. These events were mainly related to supercontinent formation, as observed elsewhere by Bradley (2011). Accordingly, in the Svecfennian orogen, LCT pegmatite ages are 1.8–1.79 Ga. This suggests relatively late emplacement in the orogenic cycle that postdated arc accretion and the first regional metamorphism, and might be related to crustal thickening as well as to a late amphibolite-facies metamorphic event.

During the Sveconorwegian orogen, emplacement of Li-rich pegmatites (910–906 Ma) appears coeval with the late Dalane phase (970–900 Ma), corresponding to gravitational collapse and post-collisional magmatism, as well as the formation of a gneiss dome and core complex related to low pressure/high temperature metamorphism. The Scottish and ca. 412 Ma LCT pegmatites from Ireland, which are part of the Caledonian orogenic belt, appear coeval with crustal thickening and post-subduction magmatism.

In the Variscan belt, RMG (Beauvoir, Montebras and Richemont, France; Argemela, Portugal; St Austell, UK), greisen (Cligga Head, Tregonning-Godolphin, Meldon, UK; Dilha Dolina, Slovakia; Montebras, France; Krasno-Konik, Krupka, Czech Republic) and various LCT pegmatites (Table 5, Fig. 6) are widely distributed (Fig. 8). Their ages suggest mostly emplacement during the Late Carboniferous (Table 5) reflecting highly fractionated magmatic events throughout the

European core related to a post-collisional stage ending the Variscan orogeny *sensu stricto* (Fig. 6, Table 5; e.g., Bonin, 1998; Chen et al., 1993; Cuney et al., 2002; Melleton et al., 2012; Neace et al., 2016). Moreover, from the internal to the external orogenic domains Li-magmatism appears to be diachronous, indicating southward prograding Li-rich magmatic activity traversing the entire belt. In the internal zones (France, Germany, Czech Republic and NW Iberia) RMG, greisen and LCT pegmatites were mostly emplaced between 320 and 307 Ma corresponding to the Bavarian phase (330–315 Ma; Finger et al., 2007) in the Bohemian Massif and to synorogenic collapse and NW-NE stretching in the French Massif Central (320–310 Ma). In the external zones (UK, parts of Spain and Portugal), similar deposits tended to be emplaced around 305 and 301 Ma (excluding the ca. 326 Ma Argemela granite) suggesting late-orogenic magmatism (Melleton et al., 2015). Finally, deposits belonging to the Gemeric unit in the Western Carpathians of Slovakia, as well as the Austroalpine pegmatites of the Eastern Alps that form the extreme margins of the belt, indicate Permian ages coeval with regional partial melting (Finger et al., 2003; Petrik et al., 2014; Illickovic et al., 2017).

Thus, it appears that the emplacement of RMG, greisen and LCT pegmatites was relatively late in the orogenic cycle and may have been coeval with continent-continent collision, commonly postdating arc accretion. It could also be related to crustal thickening (Alviola et al., 2001), a favorable setting for crustal peraluminous melt (Cuney et al., 1992; Cuney and Alexandrov, 2002) through wall-rock assimilation, the unmixing of restite, and/or internal fluid circulation related to convective fractionation (Lehmann, 1994; Martin and De Vito, 2005).

Importantly, it also appears that the reported greisen were developed from RMG, suggesting that most of the greisen associated with fractionated S-type peraluminous granite may not show significant Li contents. The formation model involves early exsolution of an $\text{F-CO}_2\text{-H}_2\text{O}$ -rich aqueous phase from the granitic magma, along with fluid/rock interactions leading to dissolution/precipitation and re-concentration of incompatible elements, such as Li, F, Sn, W, etc., within the greisen (Heinrich, 1990). Here: 1) miarolitic cavities are common and reflect volatile saturation; and 2) a decrease in rock volume and increase of porosity are reported. In the 321.5 ± 3 Ma Cinovec deposit, dissolution of the protolithionite—formed during magmatic intrusion—and precipitation of zinnwaldite during greisenization have led to remobilization of Li into its final host mineral (Johan and Johan, 2005).

4.2. Exogenous processes related to lithium occurrences

Several Li-occurrences in Europe reflect a concentration of lithium in sedimentary rocks through various exogenous processes, such as hydrothermal circulation and/or erosion and transport. Thus, distinct occurrence types can be distinguished.

4.2.1. Jadar deposit type

The Jadar deposit type is exclusively Neogene (Oligocene to Pliocene), based on available data. The existence of several other isolated intramontane lacustrine evaporite basins is suggested in Serbia (Fig. 8) as well as in Bosnia, such as the Valjevo-Mionica or Lopare basins from where jadarite was reported. Interestingly, the subsurface of these basins includes LCT pegmatite and Cretaceous to Miocene granitic intrusions, suggesting local lithium enrichment in the basement (Stojadinovic et al., 2017). These basins were formed during the late stage of the Dinadiric orogeny (Fig. 7), coeval with the extensional collapse and back-arc extension due to Carpathian slab retreat (Simić et al., 2017).

Jadarite precipitation is poorly constrained. Some authors suggested that interaction between clastic sedimentary rocks and the surrounding brine—possibly involving hydrothermal devitrification and hydration of andesitic-dacitic pyroclastic material or alteration of clay minerals—may contribute to its precipitation (Stanley et al., 2007; Stojadinovic et al., 2017).

4.2.2. Mn-(Fe) deposits

Two distinct periods of Mn-(Fe) precipitation in Europe are described here. A first group of deposits in Scotland, Wales (e.g., Drosogl Mine), England (Clews Gill), Belgium (Ottré, Beez) and Germany (Harz) is Cambrian to Early Ordovician in age (Fig. 8; Waldron et al., 2011; Romer et al., 2011), representing a notable relic of the Cadomian orogeny (650–550 Ma; Fig. 4). They are exclusively located in the Avalonian plate, constrained by the Rheic Suture, and are formed from weathering of the Cadomian magmatic arc of the Gondwana plate, as suggested by Nd and Sr isotopes (Romer et al., 2011). Interestingly, in Europe, the Cadomian orogeny was subsequently reworked during the Caledonian and Variscan orogenies (Zelazniewicz et al., 1997; Melleton et al., 2012).

The second group is mainly found in Hungary, where the Eplény and Urkút Mn deposits are Jurassic in age (Polgari et al., 2005; Figs. 7 and 8). These deposits are associated with marine sedimentary rocks mainly composed of bioclastic limestone and black shale.

The Li-bearing mineral lithiophorite, as most Mn- and Fe-oxides, was formed from secondary fluid circulation in the host rock (Nicholson and Anderton, 1989). Romer et al. (2011) suggested that the lithium component derived from chemical weathering of continental crust and was originally concentrated in siliciclastic or carbonate rocks. Thus, late hydrothermal fluid circulation may have remobilized—and still remobilizes—the Li_2O content via dissolution/precipitation processes, thus helping the precipitation of Li-bearing oxides under oxidizing conditions. Moreover, several authors pointed out their distribution along regional faults that are favorable sites for fluid circulation, such as the Candwr Fault in Wales (Cotterell et al., 2009) and the Red Gill Fault in the UK (Clark, 1963).

4.2.3. Bauxite deposits

Li-bearing minerals in bauxite deposits are Cretaceous in Hungary (D'argenio and Mindszenty, 1986) and Jurassic to Cretaceous in Greece where they are located along the northern shores of the Mediterranean Sea (Bardossy, 1982).

In Hungary, these deposits are stratiform where bedrock is a non-uniform karst carbonate rock, in which the bauxite horizons are relatively large. The Halimba mining district is one of the largest, with bauxite thickness varying from 1 to 40 m. Here, the Li-bearing mineral lithiophorite originated from secondary fluid circulation through the host rock (Bardossy, 1982) forming Mn-rich layers in epi- and supergene crusts. Cookeite is also reported from these deposits (Bardossy, 1982).

4.3. Discussion of rare-metal magma formation

There are currently two distinct models of rare-metal magma formation. The first one involves the escape of late-stage melts ending the crystallization of huge highly fractionated felsic magma chambers (e.g., Jahns and Burnham, 1969; London, 1992). One of the major arguments for this model is the regional zoning of pegmatite bodies in the margins of supposed parent granites (e.g., Cameron et al., 1949; Černý and Ercit, 2005). An example is the Fregeneda-Almendra pegmatite field where crystal-fractionation modelling and geochronology support a magmatic origin (Vieira, 2011; Roda-Robles et al., 2016). Moreover, the widespread presence of pegmatites and RMG in granites (e.g., London, 1992; Černý and Ercit, 2005) suggests a granite-related origin (e.g. Roda-Robles et al., 2016).

However, some aspects disagree with this model, suggesting a second model that involves low-grade partial melting of crustal sequences (e.g., Norton, 1973; Zasedatelev, 1977; Stewart, 1978; Melleton et al., 2011; Müller et al., 2015; Bongiolo et al., 2016). In southern Ireland, geochemical evidence points to the absence of a relationship between the LCT-spodumene Aclare pegmatite field and the surrounding Tullow Lowlands and Blackstairs plutons that are part of the Leinster Granite. This absence concerns their capacity of generating

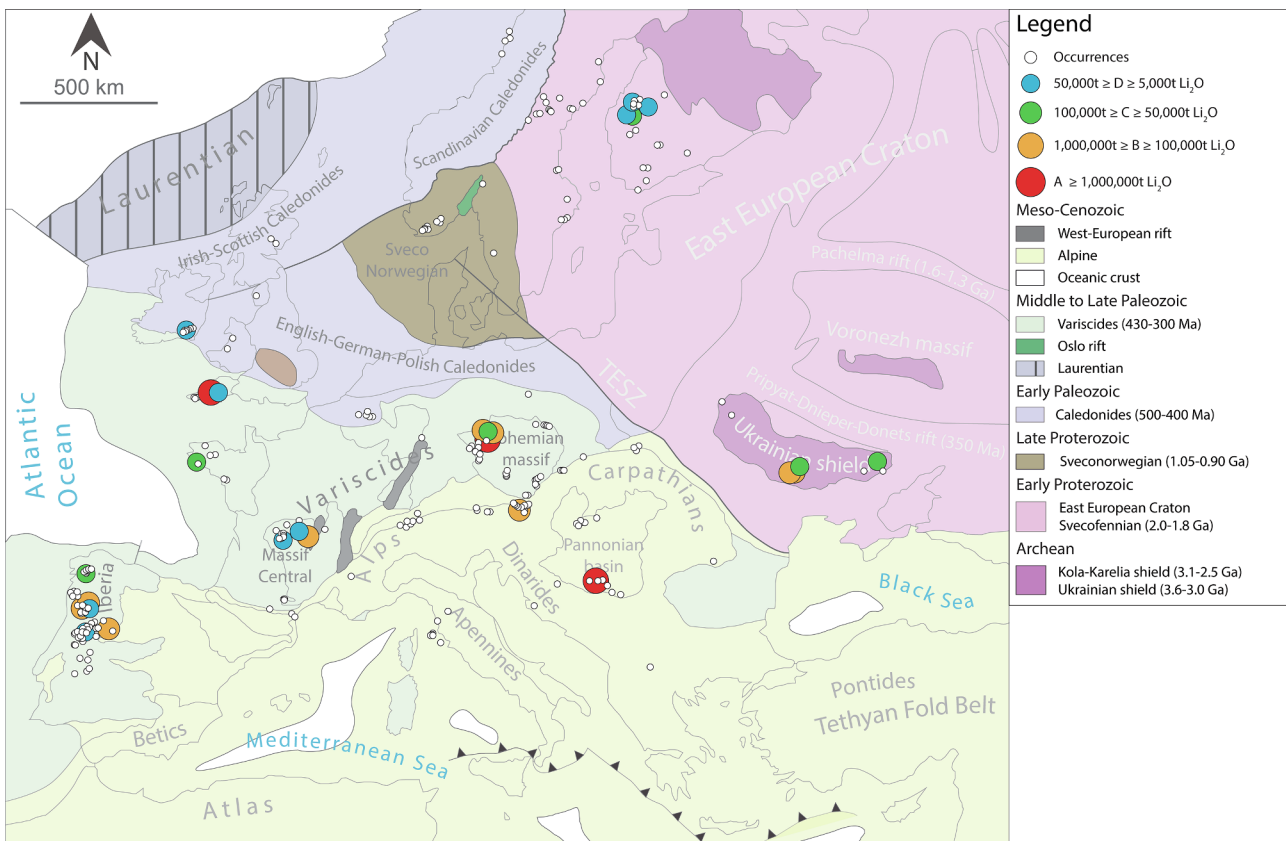


Fig. 9. Location map of the Li deposits (Table 4) in Europe (modified after Artemieva et al., 2006; Charles et al., 2013). Categories refer to: A \geq 1,000,000 t Li₂O; 1,000,000 t \geq Category B \geq 100,000 t Li₂O; 100,000 t \geq Category C \geq 50,000 t Li₂O; 50,000 t \geq Category D \geq 5000 t Li₂O; Category E < 5000 t Li₂O and past production and mineral resources.

a residual pegmatite melt (Barros et al., 2016). These authors suggested a separate partial-melting event for both units, although the intrusion of the granitic unit may have triggered anatexis of the surrounding sedimentary rocks.

In the French Massif Central, the Monts d'Ambazac pegmatite field has ^{87}Li mica values that are consistent with a crustal metasedimentary source. It is also coeval with evidence of a partial-melting event, excluding the influence of magmatic fractionation from the nearby St Sylvestre granite in the formation of pegmatites. It also demonstrates that strong Li enrichment in pegmatite is not related to a fractionation process (Deveaud et al., 2015). In the Bohemian Massif and in Austria, LCT pegmatite fields are also supposed to be formed by partial melting processes (Melleton et al., 2012).

Thus, a model of partial melting during anatexis of sedimentary rock (evaporites, cookeite-bearing metapelite, Li-rich metasedimentary rock, or Li-rich Ordovician orthogneiss, etc.) may be applied (Fig. 10), involving coeval emplacement for S-type granite (e.g., Kontak et al., 2002) and nearby LCT pegmatite, but not promoting a “parental” relationship. Moreover, micas, garnet and staurolite, which are widespread in metasedimentary rock, are seen as a potential source for lithophile elements such as Li (London, 2005, 2018). For instance, in the Brissago-Valle di Ponte area (Switzerland-Italy), poorly fractionated LCT phosphate pegmatites are suspected to be derived from local partial melting of kinzigitic during high-temperature metamorphism (Vignola et al., 2008). At the European scale, various Li-bearing minerals are reported from pegmatites, including Li-micas, lepidolite, spodumene and petalite, involving variations in the fluxing content (F, B and P) of the magmatic fluid (Roda-Robles et al., 2010), as well as varying P/T conditions (e.g., spodumene versus petalite; London, 1986, 1990). These variations are also seen in the Scandinavian orogenies, where zonation of Li-bearing minerals is highlighted: 1) the Svecfennian LCT

pegmatites are associated with Li-silicate and Li-phosphate minerals; but 2) the Sveconorwegian LCT pegmatites show a Li-phyllosilicate affinity.

4.4. From source to sink

As suggested above, several parameters may control the lithium mineralization locations in Europe. The observed clustering of endogenous lithium deposits such as LCT pegmatites, RMG and/or greisen may involve a crustal anomaly (> 20 ppm; Rudnick and Gao, 2004), or a Li “pre-concentration” related to paleoenvironmental sedimentation conditions (e.g., type of basin, host rock, climate) and/or post-deposition processes (weathering, basin-fluid circulation in the crust), more generally preserved along a paleo passive-margin (Fig. 9; Romer and Kroner, 2015).

In any case, this involves the existence of a primary Li-source that can be of magmatic origin, such as erosional material from a continental magmatic arc and related Mn(Fe) deposits and lithiophorite occurrences. Another possibility is a sedimentary origin, such as the Schist-Metagreywacke Complex in the Galicia-Trás-Os-Montes Zone (Roda-Robles et al., 2016), or the Pohjanmaa schist belt in Finland and related LCT pegmatites (Eilu et al., 2012). In that respect, significant lithospheric thickening may be favorable for concentrating Li in a specific location (Eilu et al., 2012). The occurrence of several types of Li mineralization in the French Massif Central (Fig. 6; LCT pegmatite, greisen, RMG, Li-bearing tosudite) forming clusters may suggest a possible common Li-source (Cuney and Barbey, 2014). Moreover, a recent isotopic ^{87}Li study of pegmatites (Deveaud, 2015; Deveaud et al., 2015), suggested that beryl-columbite and lepidolite-petalite LCT pegmatites from the Monts d'Ambazac show a distinct crustal contribution, indicating that Li-rich sources may contribute to “secondary” lithium

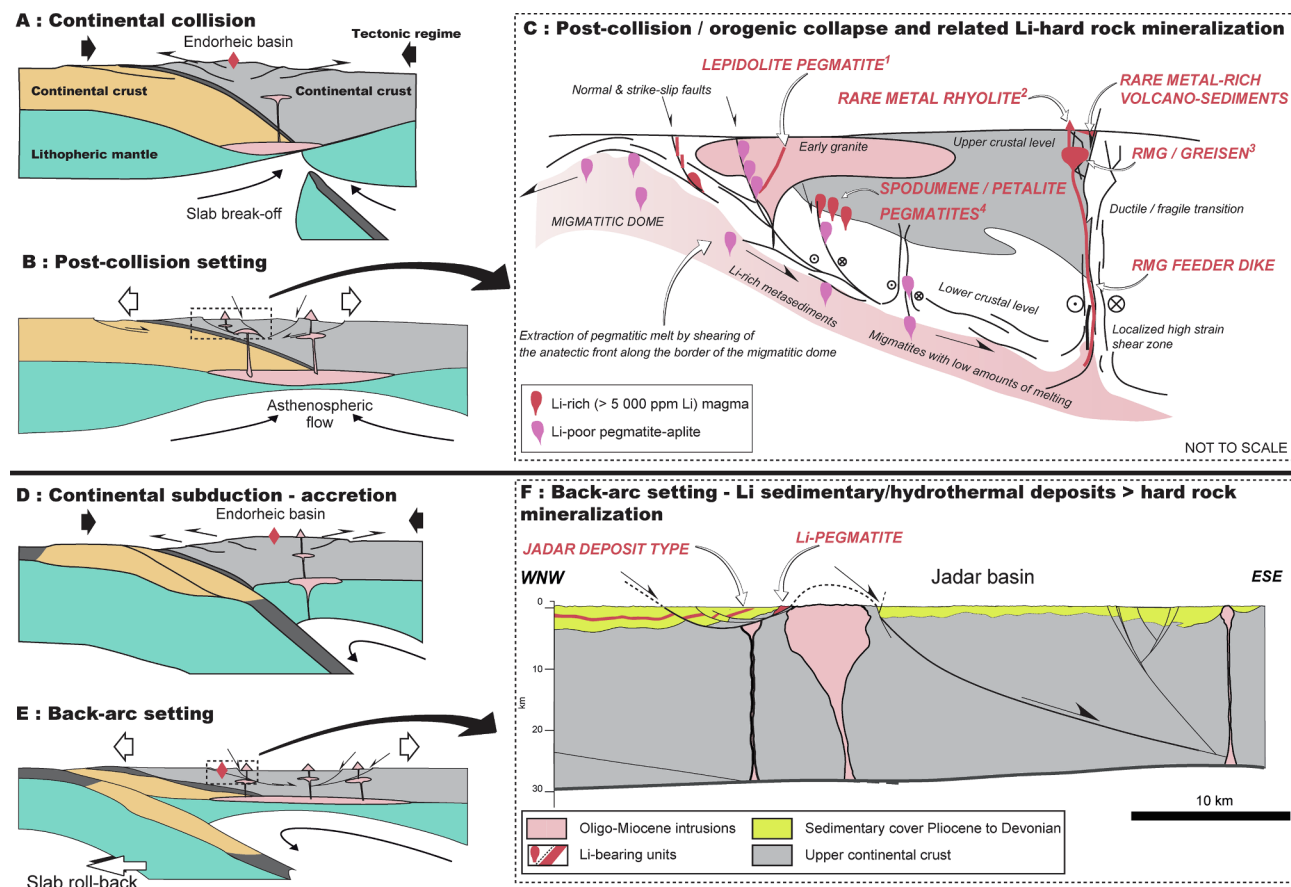


Fig. 10. Geological sections of favorable lithium setting. Continental collision (A; modified from Menant et al., 2018) shifting to post-collision setting (B; modified from Menant et al., 2018) represents favorable context for Li-hard-rock formation such as LCT pegmatites, RMG and greisen along orogenic collapse (C). Superscripts on C correspond to European examples: ¹ = Chédeville, Mina Feli, or Gonçalo; ² = Richemont; ³ = Beauvoir, Argemela and Montebras; ⁴ = Barroso-Alvao, Lânta and Aclare. Continental subduction (D; modified from Menant et al., 2018) shifting to back-arc setting (E; modified from Menant et al., 2018) represents favorable context for sedimentary/hydrothermal Li deposits such as Jadar (F; modified from Stojadinovic et al., 2017). LCT pegmatite can also occur in such a context.

deposits if suitable processes are involved.

The timing of fluid circulation appears to be another important feature for Li-concentration, whether related to a regional or to a local extensional regime in an orogenic cycle (Figs. 9 and 10; e.g., Eilu et al., 2012; Jolivet et al., 2009; Melloton et al., 2015; Stojadinovic et al., 2017; Menant et al., 2018). Sedimentary/hydrothermal lithium deposits are thus mainly related to regional extension (rifting or back-arc extension; Krone and Romer, 2013; Simić et al., 2017; Stojadinovic et al., 2017), whereas magmatic-related lithium deposits are associated with local decompression and/or transtension strike-slip deformation in late continent-continent orogenic cycles, leading to the formation of a volatile-rich melt (Fig. 10). According to Kontak et al. (2002), this melt may cause over-pressure and/or hydro-fracturing, resulting in the formation of dilatant zones and related fracture sets. Remarkably, sedimentary rocks enriched in Li during an extensional regime (e.g., Jadar Basin) may be a favorable Li source during a subsequent magmatic event. Unfortunately, a lack of data makes it impossible to confirm this hypothesis.

Finally, the distribution of Li-occurrences is strongly influenced by the location and geometry of fracture sets (Figs. 9 and 10; Deveaud et al., 2013; Deveaud, 2015; Silva et al., 2018). High permeability fractured zones seem to act as favorable channels for: 1) The emplacement of LCT pegmatite or RMG from evolved magma; or 2) Hydrothermal fluid circulation through sedimentary successions (Jadar Basin, lithiophorite occurrences in Aalenian black shales) leading to secondary Li-bearing mineral (lithiophorite, cookeite) precipitation. A recent geostatistical study showed that most pegmatites occur less than 500 m from a fault system (Deveaud et al., 2013).

4.5. Grade assessment of and tonnage estimation

4.5.1. Data quality

When regarding the available dataset, several problems are obvious. The differences in knowledge and definition of mineral resources and reserves vary between historical data (St Austell, Beauvoir), JORC (Jadar project) and NI43-101 (Alberta I project). Historical data estimates predate the CRIRSCO system (before 1995; www.crirsco.com). They are based on drilling campaigns managed by geological surveys and related subsidiaries. Such data may lead to under- or over-estimates. Fig. 11 shows that projects and occurrences are distributed homogeneously despite their reference system (historical data in italics versus CRIRSCO system in bold). Note that mineral resources from the St Austell deposits appear to be strongly anomalous from the main population (Fig. 11, Table 4); they are unrealistic for environmental and societal reasons, and probably not economically viable regarding ore grades. For these reasons, the St Austell data are not used in the following sections. The JORC system, however, may exclude some commercially sensitive information, such as mineral reserves if mineral resources (Table 4), which is not allowed with the NI43-101 report. However, these points do not affect the mineral resources comparison on which our estimates are based.

As mentioned above, thirteen projects in England (Meldon), Ireland (Aclare), France (Beauvoir, Montebras), Germany (Altenberg) and Ukraine were evaluated before setting up a “reporting system”, as such mineral resource and -reserve estimates refer to historical evaluations. These data represent only 5% of the entire dataset (Table 4). Fifteen projects were defined in the Australian JORC system (e.g., Wolfsberg,

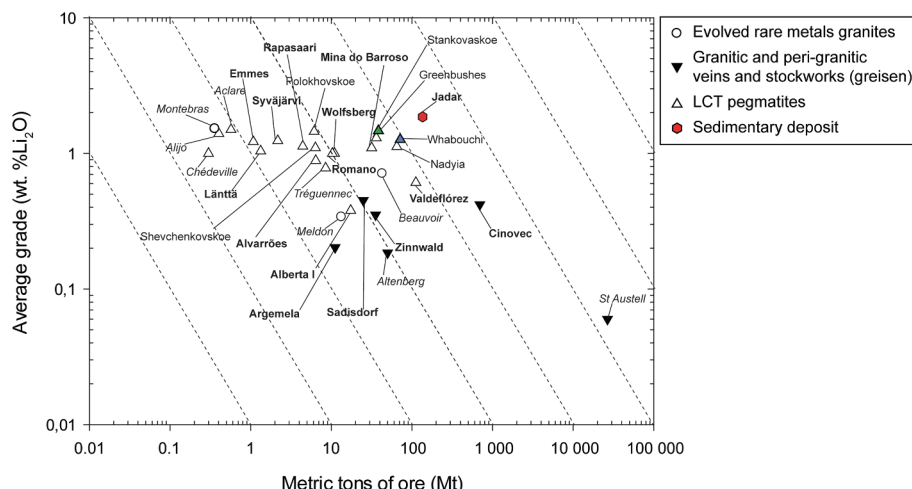


Fig. 11. Average lithium grade (wt% Li₂O) versus metric tons of ore (Mt) for the 28 identified Li deposits in Europe regarding their deposit type. Deposits and projects based on historical estimates are written in italics and those based on the CRIRSCO system in bold. The Whabouchi (Canada; blue triangle) and Greenbushes (Australia; green triangle) pegmatite deposits are mentioned here in order to compare these world-class deposits to European grades and tonnages. (For interpretation of the references to color in this figure legend, the reader is referred to the web version of this article.)

Austria); one project (Zinnwald, Germany) in the European PERC; one in the Canadian NI43-101 system (e.g., Alberta I project which comprises Presqueria deposit, Spain) and one project is defined in the United Nation Framework Classification (UNFC; Alijo deposit).

However, we think that, despite the apparent discrepancies between

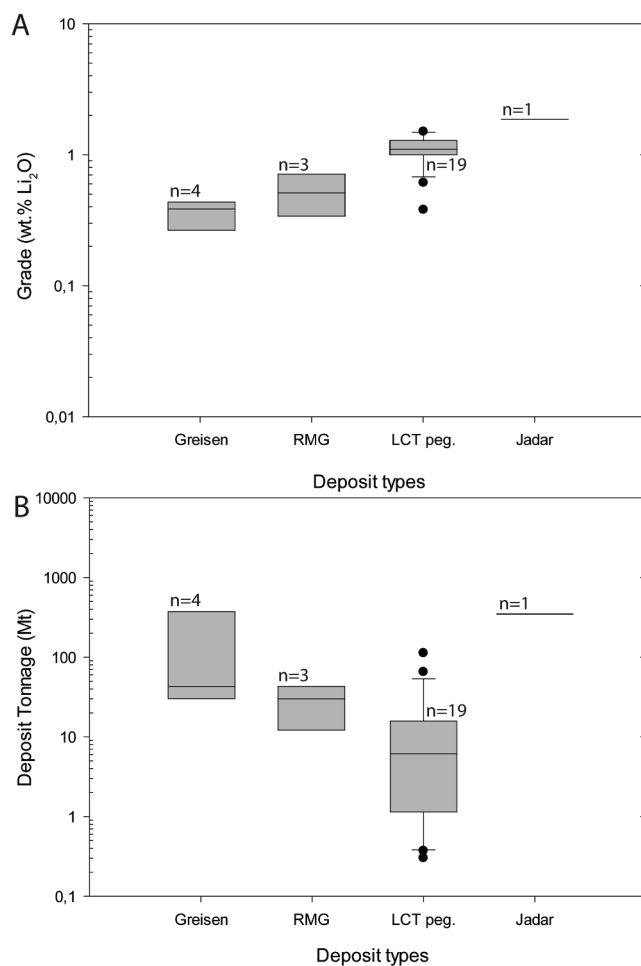


Fig. 12. Grade (wt% Li₂O) versus deposit types (A) and deposit tonnage (Mt) versus deposit types (B) considering resource estimates. The boxes indicate the median (black line), upper and lower quartiles (25%; gray boxes), maximum and minimum values (upper and lower whiskers) and outliers (black circles). Note that n reflects the total number of deposits considered for this summary plot.

reference systems, our dataset is a good starting point for estimating the European Li hard-rock potential (Figs. 11 and 12).

Moreover, Li-bearing minerals in lithiophorite and Li-chlorite occurrences in sedimentary deposits—bauxite, Mn-(Fe), MVT and Li-bearing clay deposits—were not systematically described, as Li was not of first interest at the time. This was the case in Spain, France and Turkey, and may hide significant local Li grades, as in China (Wang et al., 2013) and USA (Tourtelot and Brenner-Tourtelot, 1977). Available data from bauxite deposits in China show that the average Li grade is very low (2045 ppm Li₂O; Wang et al., 2013). The same is true for Li-bearing shales in the Dauphinois area, France, where the average Li content is 949.34 ppm Li₂O (Henry et al., 1996). Accordingly, these occurrences can hardly be considered as potential Li deposits regarding their ore grade.

Based on the available dataset, 8,839,750 t of Li₂O (Table 4) are presently reported in Europe from various deposit types and related to various Li-bearing minerals.

Furthermore, our study does not cover lithium in seawater, whose average content has been estimated at 0.17 ppm (Fasel and Tran, 2005; Yaksic and Tilton, 2009), nor that potentially contained in oilfields (e.g., Pechelbronn in France) and geothermal brines (e.g., the South Crofty deposit in the UK; Cornish Lithium/Strongbow). Such potential lithium sources are difficult to quantify due to fluid mixing, dilution and/or movement (Houston et al., 2011), but research is ongoing (e.g., Eramet-IFPEN), as are potential resource estimates from such sources.

4.5.2. Range of ore grade and tonnage

At the deposit scale, metric tons of ore and average grades (Fig. 11, Table 4) of European hard-rock lithium deposits are relatively competitive compared to the world-class LCT pegmatites from the Greenbushes in Australia and Whabouchi in Canada, which are representative examples of such Li-deposits. In detail, the Proterozoic Ukrainian pegmatites show similar grades and tonnages, whereas Variscan pegmatites host lower tonnages. Thus, as pointed out before, significant differences in Li content are seen among the various orogens. Interestingly, the Svecocennian, Sveconorwegian and Variscan orogenies, which involved supercontinent accretion, continent-continent collision and notable late lithospheric thickening, resulted in richer lithium deposits than the Cadomian, Caledonian and Alpine orogenies. This suggests that processes involving extensive crustal anatexis from lithospheric thickening lead to significant Li enrichment (Černý, 1991a,b). For the Apine orogen, the dearth in Li deposits could be related to a present-day deep erosional level, as indicated by the presence of few LCT pegmatites emplaced at the highest structural levels, highlighted by miarolitic (Guastoni et al., 2014, Guastoni et al., 2016) features (MI class of

Cerný and Ercit, 2005).

It also appears that greisen and RMG containing mainly Li-micas (lepidolite, zinnwaldite, Li-muscovite) and Li-phosphates, may contain relatively higher tonnages, but lower grades, than the LCT pegmatites, which contain mainly spodumene- and petalite-dominated Li-bearing minerals (Figs. 11 and 12). This is, first, a function of deposit size: pegmatites are narrow and well constrained whereas greisen and RMG can form kilometer-scale cupolas and may have deep roots (e.g., Beauvoir). Second, the type of Li-bearing mineral, within which the Li_2O content may vary significantly (Table 1), is another major parameter, illustrated by spodumene versus zinnwaldite.

Finally, in addition to the above points, ore grade can be controlled by several other parameters. These include the geochemistry of fluxing fluids (F, B and P), different crystallization parameters and P-T conditions (spodumene versus petalite; Černý and Ferguson, 1972), and variable degrees of fractionation (Li-phosphate occurrences against amblygonite-montebrasite or triphyllite-sicklerite-ferrisicklerite series; Černý, 1991b). All these may affect the number and type of Li-bearing minerals, as well as their mineral size and relative abundance, and therefore the overall Li content.

4.6. Perspectives

As emphasized by this study, lithium in hard-rock deposits is not rare in Europe and well distributed within Proterozoic to Cenozoic orogens (Fig. 8). The Variscan orogeny (Fig. 6) shows the most important Li-content (> 60% of the identified deposits in Table 4) in various deposit types (greisen, RMG, pegmatite). The oldest orogens mainly contain LCT pegmatites (Figs. 3 and 5) that tend to cluster, potentially because of successive orogenic reworking. However, only very few studies report lithium occurrences related to young Mediterranean orogens, suggesting either a lack of exploration or a significant difference between the Variscan and Alpine orogenies.

As for jadarite occurrences, greenfield exploration in Balkan countries such as Serbia and Bosnia may identify latent deposits related to lacustrine evaporite basins. Currently, this area is relatively under-explored and several exploration and mining companies showed recent interest in acquiring permits, such as the Australian firm South East Asia Resources, recently renamed Jadar Lithium.

Regarding Li-production, LCT pegmatites that generally have high lithium grades and low tonnages could be rapidly in production as Li-extraction processes for spodumene are operational. Greisen and RMG, which have low Li grades and high tonnages, will take somewhat longer to reach production as the extraction processes of Li-bearing micas must be demonstrated at deposit scale.

5. Conclusions

This review of Li hard-rock lithium metallogeny in Europe demonstrates that a wide range of deposit types, including endogenous (LCT pegmatites, RMG, greisen) and exogenous (Jadar, bauxite) processes, is involved. The lithium is contained in various Li-bearing minerals, such as spodumene, lepidolite and zinnwaldite, which are related to different orogenies through time. A favorable geodynamic setting for endogenous magmatic lithium accumulation comprises a late orogenic process, commonly postdating arc accretion, coeval with continent-continent collision, and related to local crustal thickening. A post-orogenic extensional setting is favorable for exogenous processes that can concentrate lithium into a deposit.

At present, 27 potential hard-rock deposits have been identified in Europe. The sum of such Li resources is estimated at 8,839,750 t of Li_2O . Their production may secure, in part, European lithium requirements in the near future.

Our inventory also reflects the heterogeneity in knowledge regarding lithium occurrences. This is due to a relative lack of interest in lithium until recently and suggests that new targets might be defined in

the foreseeable future through active ongoing exploration.

Acknowledgements

We gratefully acknowledge Drs. Mali H., Uher P., and Ilickovic T. for their assistance regarding European occurrence locations. We also thank Matevž Novak from the Geological Survey of Slovenia for the use of the jadarite picture. This study was funded by the French Centre for Excellence Voltaire* – LABEX VOLTAIRE (Geofluids and VOLatils, Earth, Atmosphere – Resources and Environment) in collaboration with the French geological survey (BRGM) and the Economic Laboratory of Orléans University (LEO). We thank three anonymous reviewers and Dr. Seltmann for their constructive comments that greatly helped to improve the manuscript. Dr. H.M. Kluijver edited the final English version of the manuscript.

Appendix A. Supplementary data

Supplementary data to this article can be found online at <https://doi.org/10.1016/j.oregeorev.2019.04.015>.

References

- Ackerman, L., Haluzová, E., Creaser, R.A., Pašava, J., Veselovský, F., Breiter, K., Erban, V., Drábek, M., 2017. Temporal evolution of mineralization events in the Bohemian Massif inferred from the Re-Os geochronology of molybdenite. Miner. Deposita 52, 651–662. <https://doi.org/10.1007/s00126-016-0685-5>.
- Alviola, R., Mänttäri, I., Mäkitie, H., Vaasjoki, M., 2001. Svecofennian rare-element granitic pegmatites of the Ostrobothnia region, western Finland: their metamorphic environment and time of intrusion. Geological Survey of Finland. Special Paper 30, pp. 9–29.
- Anderson, S.T., 2015. . The mineral Industry of Hungary. In: 2012 Yearbook, Hungary. USGS Science for a changing world, pp. 8.
- Armand, M., Tarascon, J.M., 2008. Building better batteries. Nature 451, 652–657.
- Artemieva, I.M., Thybo, H., Kaban, M.K., 2006. Deep Europe today: geophysical synthesis of the upper mantle structure and lithospheric processes over 3.5 Ga. Mem. Geol. Soc. London 32, 11–41.
- Artemieva, I.M., Thybo, H., 2013. EUNAseis: A seismic model for Moho and crustal structure in Europe, Greenland, and the North Atlantic region. Tectonophysics 609, 97–153.
- Aubert, G., 1969. Les coupoles granitiques de Montebbras et d'Echassières (Massif Central français) et la genèse de leurs minéralisations en étain, lithium, tungstène et beryllium. Mémoire BRGM 46, 345 pp.
- Bardossy, G., 1982. Karst bauxites, Bauxite deposits on carbonate rocks. In: Developments in economic geology. Elsevier Scientific publishing company, pp. 442.
- Barros, R., 2017. Petrogenesis of the Leinster LCT (Li-Cs-Ta) pegmatite belt in southeast Ireland. PhD Thesis. University College Dublin, pp. Ireland287.
- Barros, R., Menoge, J.F., 2016. The origin of spodumene pegmatites associated with the Leinster granite in southeast Ireland. Can. Mineral. 54, 847–862.
- Belteraldo, M., Frasca, G., Compagnoni, R., Vitale-Brovarone, A., 2012. The Valaisian controversy revisited: multi-stage folding of a Mesozoic hyper-extended margin in the Petit St. Bernard pass area (Western Alps). Tectonophysics 579, 17–36.
- Bergh, S.G., Corfu, F., Priyatrina, N., Kullerud, K., Myhre, P.I., 2015. Multiple post-Svecofennian 1750–1560 Ma pegmatite dykes in Archean-Paleoproterozoic rocks of the West Troms Basement Complex, North Norway: geological significance and regional implications. Precambrian Res. 266, 425–439.
- Bertotti, G., Seward, D., Wijbrans, J., Ter Voorde, M., Hurford, A.J., 1999. Crustal thermal regime prior to, during, and after rifting: a geochronological and modelling study of the Mesozoic South Alpine rifted margin. Tectonics 18, 185–200.
- Bingen, B., Davis, W.J., Hamilton, M.A., Engvik, A.K., Stein, H.J., Skar, O., Nordgulen, O., 2008a. Geochronology of high grade metamorphism in the Sveconorwegian belt, S. Norway: U-Pb, Th-Pb and Re-Os data. Nor. J. Geol. 88, 13–40.
- Bingen, B., Nordgulen, O., Viola, G., 2008b. A four-phase model for the Sveconorwegian orogeny SW Scandinavia. Nor. J. Geol. 88, 43–72.
- Bongiolo, E.M., Renac, C., de Toledo, d'Almeida, Piza, P., da Silva Schmitt, R., Sampaio, Mexias A., 2016. Origin of pegmatites and fluids at Ponta Negra (RJ, Brazil) during late to post-collisional stages of the Gondwana Assembly. Lithos 240–243, 259–275.
- Bonin, B., 1998. Orogenic to non-orogenic magmatic events: Overview of the Late Variscan magmatic evolution of the Alpine Belt. Turk. J. Earth Sci. 7, 133–143.
- Bousquet, R., Schmid, S.M., Zeilinger, G.R., Rosenberg, C., Molli, G., Robert, C., Wiederkehr, M., Rossi, P., 2012. Tectonic framework of the Alps, Scale 1:1,000,000. Commission for the Geological Map of the World.
- Bradley, D.C., Munk, L., Jochens, H., Hynek, S., Labay, K., 2013. A preliminary deposit model for lithium brines. U.S. Geological Survey, Open File Report 2013-1006, 9.
- Bradley, D.C., 2011. Secular trends in the geologic record and the supercontinent cycle. Earth-Sci. Rev. 108, 16–33.
- Braux, C., Piantone, P., Zeegers, H., Bonnemaison, M., Prévot, J.C., 1993. Le Châtelet gold-bearing arsenopyrite deposit, Massif Central France: Mineralogy and geochemistry applied to prospecting. Appl. Geochem. 8, 339–356.
- Breiter, K., Korbeloca, Z., Chladek, S., Uher, P., Knesl, I., Rambousek, P., Honig, S., Sesulka, V., 2017. Diversity of Ti-Sn-W-Nb-Ta oxide minerals in the classic granite-related magmatic-hydrothermal Cinovec/Zinnwald Sn-W-Li deposit (Czech

- Republic). *Eur. J. Mineral.* 29, 727–738.
- BRGM, 2017. Le lithium (Li) – éléments de criticité, fiche de synthèse sur la criticité des matières minérales – le lithium. *Mineral Info* 8.
- British Geological Survey, 2016. Lithium. Minerals UK, Mineral profile, pp. 39.
- Brown, D., Juhlin, C., Ayala, C., Tryggvason, A., Bea, F., Alvarez-Marron, J., Carbonell, R., Seward, D., Glasmacher, U., Puchkov, V., Perez-Estaun, A., 2008. Mountain building processes during continent–continent collision in the Uralides. *Earth-Sci. Rev.* 89, 177–195.
- Bussink, R.W., 1984. PhD thesis In: *Geochemistry of the Panasqueira tungsten-tin deposit*, Portugal. University of Utrecht, The Netherlands, pp. 170.
- Cameron, E.N., Jahns, R.H., McNair, A.H., Page, L.R., 1949. Internal structure of granitic pegmatites. *Econ. Geol. Monogr.* 2, 115 p.
- Cassard, D., Bertrand, G., Billia, M., Serrano, J.J., Tourrière, B., Angel, J.M., Gaa, G., 2015. ProMine Mineral Databases: New tools to assess primary and secondary mineral resources. In: 3D, 4D and Predictive Modelling of Major Mineral Belts in Europe, Weihs P., (ed.); *Mineral Resource Reviews*, DOI 10.1007/978-3-319-17428-0_2.
- Černý, P., 1992. Regional zoning of pegmatite populations and its interpretation. *Mitt. der Österreichischen Mineralogischen Ges.* 137, 99–107.
- Černý, P., 1991a. Rare-element granitic pegmatites. Part 1: Anatomy and internal evolution of pegmatite deposits. *Geosci. Can.* 18, 49–67.
- Černý, P., 1991b. Rare-element granitic pegmatites. Part 2: Regional to global environments and petrogenesis. *Geosci. Can.* 18, 68–81.
- Černý, P., 1990. Distribution, affiliation and derivation of rare-element granitic pegmatites in the Canadian Shield. *Geol. Rundschau* 79, 183–226.
- Černý, P., 1989. Characteristics of pegmatite deposits of tantalum. Society for Geology applied to Mineral Deposits, Special Publication 7, Springer-Verlag, pp. 192–236.
- Černý, P., Ercit, T.S., 2005. The classification of granitic pegmatites revisited. *Can. Mineral.* 43, 2005–2026.
- Černý, P., Ferguson, R.B., 1972. The Tanco pegmatite at Bernic Lake, Manitoba. IV. Petalite and Spodumene relations. *Can. Mineral.* 11, 660–678.
- Černý, P., London, D., Novák, M., 2012. Granitic pegmatites as reflections of their sources. *Elements* 8, 289–294.
- Cháb, J., 2010. Outline of the geology of the Bohemian Massif: The basement rocks and their Carboniferous and Permian cover. Czech Geological Survey, Prague, pp. 295.
- Charles, N., Tuduri, J., Guyonnet, D., Melletton, J., Pourret, O., 2013. Rare earth elements in Europe and Greenland: a geological potential? An overview. *Mineral Deposit Research for a High-Tech World*, 12th SGA Biennial Meeting 4, 4.
- Chároy, B., Noronha, F., 1996. Multistage growth of rare-element, volatile-rich micro-granite at Argemela (Portugal). *J. Petrol.* 37, 73–94.
- Chároy, B., Noronha, F., 1991. The Argemela granite-porphyry (Central Portugal): the subvolcanic expression of a high-fluorine, rare-element pegmatite magma. In: *Source, Transport and deposition for metals*, Pagel M., and Leroy J.L., (Eds.), 741–744.
- Chen, Y., Clark, A.H., Farrar, E., Wasteneys, H.A., Hodgson, M.J., Bromley, A.V., 1993. Diachronous and independent histories of plutonism and mineralization in the Cornubian Batholith, southwest England. *J. Geol. Soc.*, London 150, 1183–1191.
- Christman, P., Gloaguen, E., Labbé, J.F., Melletton, J., Piantone, P., 2015. Global lithium resources and sustainability issues. Elsevier, pp. 1–40.
- Clark, L., 1963. The geology and petrology of the Ennerdale granophyre. Its metamorphic aureole and associated mineralization. PhD thesis. University of Leeds, England, pp. 324.
- Cotterell, T., 2009. Supergene manganese mineralization associated with the Camdwr fault in the Central Wales orefield. *J. Russell Soc.* 12, 15–25.
- Cuney, M., Autran, A., 1987. Objectifs généraux du projet GPF Echassières n°1 et résultats essentiels acquis par le forage de 900 m sur le granite albítique à topaze-lépidolite de Beauvoir. In: Cuney, M., Autran, A. (Eds.), Echassières. Le forage scientifique d'Echassières: une clé pour la compréhension des mécanismes magmatiques et hydrothermaux associés aux granites à métaux rares. Mémoire Géologie de la France (GPF), pp. 7–24.
- Cuney, M., Barbeay, P., 2014. Uranium, rare metals, and granulite-facies metamorphism. *Geosci. Front.* 5, 1–17.
- Cuney, M., Marignac, C., Weisbrod, A., 1992. The Beauvoir topaz-lepidolite albite granite (Massif Central, France): The disseminated magmatic Sn-Li-Ta-Nb-Be mineralization. *Econ. Geol.* 87, 1766–1794.
- Cuney, M., Alexandrov, P., Carlier, Le, de Veslud, C., Cheilletz, A., Raimbault, L., Ruffet, G., Scaillet, S., 2002. The timing of W-Sn –rare metals mineral deposit formation in the Western Variscan chain in their orogenic setting: the case of the Limousin area (Massif Central, France). Special Publications. Geological Society, London, pp. 213–228.
- Dakota Minerals Ltd., 2017. Sepeda – Largest Pegmatite-Hosted JORC Lithium Resource in Europe; ASX announcement, 20 February 2017; press release, 29 p.
- D'Argenio, B., Mindszenty, A., 1986. Cretaceous bauxites in the tectonic framework of the Mediterranean. *Rendiconti della Società Geologica Italiana di Mineralogia e Petrologia* 9, 257–262.
- Deveaud, S., Millot, R., Villars, A., 2015. The genesis of LCT-type granitic pegmatites, as illustrated by lithium isotopes in micas. *Chem. Geol.* 411, 97–101.
- Deveaud, S., 2015. PhD thesis In: *Caractérisation de la mise en place des champs de pegmatites à éléments rares de type LCT – Exemples représentatifs de la chaîne Varisque*. University of Orléans, France, pp. 350.
- Deveaud, S., Gumiäx, C., Gloaguen, E., Branquet, Y., 2013a. Spatial statistical analysis applied to rare-elements LCT pegmatite fields: An original approach to constrain fault-pegmatites-granites relationships. In: *PEG 2013, 6th International Symposium on Granitic Pegmatites*, Program with abstract, pp. 36.
- Deveaud, S., Gumiäx, C., Gloaguen, E., Branquet, Y., 2013b. Spatial statistical analysis applied to rare-element LCT type pegmatite fields: an original approach to constrain faults-pegmatites-granites relationships. *J. Geosci.* 58, 163–182.
- Elilu, P., Ahtola, T., Äikäs, O., Halooaho, T., Heikura, P., Hulkki, H., Iljina, M., Juopperi, H., Karinen, T., Kärkkäinen, N., Kununaho, J., Kontinen, A., Kontoniemi, O., Korkiakoski, E., Korsakova, M., Kuivasaari, T., Kyläkoski, M., Makkonen, H., Niiranen, T., Nikander, J., Nykänen, V., Perdahl, J.A., Pohjolainen, E., Räsänen, J., Sorjonen-Ward, P., Tiainen, M., Tontti, M., Torppa, A., Väistö, K., 2012. Metallogenetic areas in Finland. *Geol. Surv. Finland, Special Paper* 53, 207–342.
- Erickson, G.E., Salas, R., 1987. Geology and resources of salars in the central Andes. U.S. Geological Survey, Open File Report. 88-210, 51.
- Ertl, A., Schuster, R., Hughes, J.M., Ludwig, T., Meyer, H.P., Finger, F., Dyar, M.D., Ruschel, K., Rossman, G.R., Klötzli, U., Brandstätter, F., Lengauer, C.L., Tillmanns, E., 2012. Li-bearing tourmalines in Variscan granitic pegmatites from the Moldanubian nappes, Lower Austria. *Eur. J. Mineral.* 24, 695–715.
- Fasel, D., Tran, M.Q., 2005. Availability of lithium in the context of future D-T fusion reactors. *Fusion Eng. Des.* 75–79, 1163–1168.
- Faure, M., Bé Mézène, E., Duguet, M., Cartier, C., Talbot, J.Y., 2005. Paleozoic tectonic evolution of Medio-Europa from the example of the French Massif Central and Massif Armorican. *J. Virtual Explorer* 19, 26.
- Ferrara, G., Tonarini, S., 1985. Radiometric geochronology in Tuscany: results and problems. *Rend. Della Società Italiana di Mineralogia e Petrologia* 40, 111–124.
- Fritschle, T., 2016. PhD thesis. Age and origin of late Caledonian granites and Ordovician arc magmatic rocks in Ireland and the Isle of Man 359.
- Finger, F., Gerdes, A., Janousek, V., René, M., Riegler, G., 2007. Resolving the Variscan evolution of the Moldanubian sector of the Bohemian Massif: the significance of the Bavarian and the Moravuo-Moldanubian tectonometamorphic phases. *J. Geosci.* 52, 9–28.
- Finger, F., Broska, I., Haunschmid, B., Hrasko, L., Kohút, M., Krenn, E., Petrík, I., Riegler, G., 2003. Cassiterite U-Pb geochronology constrains magmatic-hydrothermal evolution in complex evolved granite systems: The classic Erzgebirge Tin Province (Saxony and Bohemia) Electron-microprobe dating of monazites from Western Carpathian basement granitoids: plutonic evidence for an important Permian rifting event subsequent to Variscan crustal anatexis. *Int. J. Earth Sci.* 92, 86–98.
- Garfunkel, Z., 2015. The relations between Gondwana and the adjacent peripheral Cadomian domain-constraints on the origin, history and paleogeography of the peripheral domain. *Gondwana Res.* 28, 1257–1281.
- Gébelin, A., Roger, F., Brunel, M., 2009. Syntectonic crustal melting and high-grade metamorphism in a transpressional regime, Variscan Massif Central, France. *Tectonophysics* 477 (3–4), 229–243. <https://doi.org/10.1016/j.tecto.2009.03.022>.
- Gébelin, A., Brunel, M., Monié, P., Faure, M., Arnaud, N., 2007. Transpressional tectonics and Carboniferous magnetism in the Limousin, Massif Central, France: structural and ⁴⁰Ar/³⁹Ar Investigations. *Tectonics* 26, 2, 27. <https://doi.org/10.1029/2005TC001822>.
- Gee, D.G., Bogolepova, O.K., Lorenz, H., 2006. The Timanide, Caledonide and Uralide orogens in the Eurasian high Arctic, and relationships to the palaeo-continents Laurentia, Baltica and Siberia. Geological Society, London, Memoirs, pp. 507–521.
- Glanzman, R.K., McCarthy Jr., J.H., Rytyba, J.J., 1978. Lithium in the McDermitt Caldera, Nevada and Oregon. *Energy* 3, 347–353.
- Gloaguen, E., Melletton, J., Lefebvre, G., Tourrière, B., Yart, S., Gourcerol, B., 2018. Ressources métropolitaines en lithium et analyse du potentiel par méthodes de prédictivité; Rapport BRGM/RP-68321-FR, 129p.
- Guastoni, A., Pozzi, G., Secco, L., Schiazza, M., Pennacchioni, G., Fioretti, A.M., Nestola, F., 2016. Monazite-(Ce) and xenotime-(Y) from an LCT, NYF tertiary pegmatite field: evidence from a regional study in the Central Alps (Italy and Switzerland). *Can. Mineral.* 54, 863–877.
- Guastoni, A., Pennacchioni, G., Pozzi, G., Fioretti, A.M., Walter, J.M., 2014. Tertiary pegmatite dikes of the Central Alps. *Can. Mineral.* 52, 191–219.
- Heinrich, C.A., 1990. The chemistry of hydrothermal tin (-tungsten) ore deposition. *Econ. Geol.* 85, 457–481.
- Henry, C., Burkhard, M., Goffré, B., 1996. Evolution of synmetamorphic veins and their wallrocks through a Western Alps transect: no evidence for large-scale flow. Stable isotope, major- and trace-element systematics. *Chem. Geol.* 127, 81–109.
- Hofstra, A.H., Todorov, T., Mercer, C., Adams, D., Marsh, E., 2013. Silicate melt inclusion evidence for extreme pre-eruptive enrichment and post-eruptive depletion of lithium in silicic volcanic rocks of the Western United States: Implications for the origin of lithium-rich brines. *Econ. Geol.* 108, 1691–1701.
- Hollinger, P., Cuney, M., Friedrich, M., Turpin, L., 1986. Age carbonifère de l'unité de Brême du complexe granitique perléumineux de Saint-Sylvestre (NO du Massif Central) défini par les données isotopiques U-Pb sur zircon et monazite. Académie des Sciences, Comptes Rendus, Series II 303, 1309–1314.
- Houston, J., Butcher, A., Ehren, P., Evans, K., Godfrey, L., 2011. The evaluation of brine prospects and the requirement for modifications to filing standards. *Econ. Geol.* 106, 1225–1239.
- Ilickovic, T., Schuster, R., Mali, H., Petrákakis, K., Schedl, A., Horschinegg, M., 2016. Spodumene bearing pegmatites in the Austroalpine unit (Eastern Alps): New field observations and geochronological data. *GeoTiro!, Abstract with Poster*, pp. 138.
- Ilickovic, T., Schuster, R., Mali, H., Petrákakis, K., Schedl, A., 2017. Spodumene bearing pegmatites in the Austroalpine unit (Eastern Alps): Distribution and new geochronological data. *Geophysical Research Abstracts*, EGU2017-7235 19 Program with Abstract.
- Jackson, B., 1982. An occurrence of gem quality elbaite from Glenbuchat, Aberdeenshire, Scotland. *J. Gemmol.* 2, 121–125.
- Jahns, R.H., Burnham, C.W., 1969. Experimental studies of pegmatites gneiss: a model for the derivation and crystallization of granitic pegmatites. *Econ. Geol.* 64, 843–864.
- Jarchovský, T., 2006. The nature and genesis of greisen stocks at Krasno, Slavkovský les area – western Bohemia, Czech Republic. *J. Czech Geol. Soc.* 51, 16.
- Johan, Z., Johan, V., 2005. Accessory minerals of the Cinovec (Zinnwald) granite cupola, Czech Republic: Indicators of petrogenetic evolution. *Mineral. Petrol.* 83, 113–150.
- Jolivet, L., Faccenna, C., Piromallo, C., 2009. From mantle to crust: Stretching the Mediterranean. *Earth Planetary Sci. Lett.* 285, 198–209.
- Johnson, T.E., Hudson, N.F.C., Droop, G.T.R., 2001. Melt segregation structures within the Inzie Head gneisses of the northeastern Daldanian. *Scott. J. Geol.* 37, 59–72.
- Jullien, M., Goffé, B., 1993. Occurrences de cookéite et de pyrophyllite dans les schistes du Dauphiné (Isère, France) – Conséquences sur la répartition du métamorphisme dans les zones extremes alpines. *Schweiz. Mineral. Petrol.* 73, 357–363.
- Kesler, S.E., Gruber, P.W., Medina, P.A., Keoleian, G.A., Everson, M.P., Wallington, T.J.,

2012. Global lithium resources: relative importance of pegmatite, brine and other deposits. *Ore Geol. Rev.* 48, 55–69.
- Kohút, M., Stein, H., 2004. Re-Os molybdenite dating of granite-related Sn-W-Mo mineralisation at Hnilec, Gemerík Superunit, Slovakia. *Mineral. Petrol.* 85, 117–129.
- Koistinen, T., Stephens, M.B., Bogatchev, V., Nordgulen, Ø., Wennerström, M., Korhonen, J., 2001. Geological Map of the Fennoscandian Shield, Scale 1:2,000,000; Espoo, Geological Survey Finland, Geological Survey Norway, Geological Survey Sweden, Ministry of Natural Resources of Russia, Moscow.
- Kontak, D.J., Dostal, J., Kyser, T.K., Archibald, D.A., 2002. A petrological, geochemical, isotopic and fluid inclusion study of 370 Ma pegmatite-aplite sheets, Peggy's Cove, Nova Scotia, Canada. *Can. Mineral.* 40, 1249–1286.
- Korja, A., Lahtinen, R., Nironen, M., 2006. The Svecocenonian orogen—a collage of microcontinents and island arcs. Geological Society, London, Memoirs, pp. 561–578.
- Kovács, I., Csontos, L., Szabó, C., Bali, E., Falus, G., Benedek, K., Zajacz, Z., 2007. Paleogene-Early Miocene igneous rocks and geodynamics of the Alpine-Carpathian-Pannonic-Dinaric region: an integrated approach. *Geol. Soc. Am. Special Paper* 41, 93.
- Kroner, U., Romer, R.L., 2013. Two plates – Many subduction zones: The Variscan orogeny reconsidered. *Gondwana Res.* 24, 298–329.
- Kulp, J.L., Kologrivov, R., Engels, J., Catanzaro, E.J., Neumann, H., Nilssen, B., 1963. Age of the Tordal, Norway pegmatite – a correction. *Geochimica et Cosmochimica Acta* 27, 847–848.
- Kuusela, J., Ahtola, T., Koistinen, E., Seppänen, H., Hatakka, T., Lohva, J., 2011. Report of investigations on the Rapasaret lithium pegmatite deposit in Kaustinen-Kokkola, Western Finland. GTK Southern Finland Office, 42/2011 65.
- Kurhila, M., Vaasjoki, M., Määttäri, I., Rämö, T., Nironen, M., 2005. U-Pb ages and Nd isotope characteristics of the late orogenic, migmatizing microcline granites in southwestern Finland. *Bull. Geol. Soc. Finland* 77, 105–128.
- Kvasnista, V.N., Silaev, V.I., Smoleva, I.V., 2016. Carbon isotopic composition of diamonds in Ukraine and their probable polygenetic nature. *Geochem. Int.* 54, 948–963.
- Lahti, S.I., 1981. On the granitic pegmatites of the Erjärvi area in Orivesi Southern Finland. *Geol. Surv. Finl. Bull.* 314, 89.
- Lahtinen, R., Korja, A., Nironen, M., Heikkilä, P., 2009. Palaeoproterozoic accretionary processes in Fennoscandia. *Geol. Soc. London, Special Publications* 318, 237–256. <https://doi.org/10.1144/SP318.8>.
- Launay, G., Sizaret, S., Guillou-Frottier, L., Fauguerolles, C., Champallier, R., Gloaguen, E., 2019. Dynamic permeability related to greisenization reactions in Sn-W ore deposits: quantitative petrophysical and experimental evidence. *Geofluids* 2019, 23p.
- Lecomte, A., Cathelineau, M., Deloule, E., Brouaud, M., Peiffert, C., Loukola-Ruskeeniemi, K., Pohjolainen, E., Lahtinen, H., 2014. Uraniferous bitumen nodules in the Talvivaara Ni-Zn-Cu-Co deposit (Finland): influence of metamorphism on uranium mineralization in black shales. *Miner. Deposita* 49, 513–533.
- Lehmann, B., 1994. Granite-related rare-metal mineralization: a general geochemical framework. *Czech Geological Survey, Prague*, pp. 342–349.
- Li, Z.X., Bogdanova, S.V., Collins, A.S., Davidson, A., de Waele, B., Ernst, R.E., et al., 2008. Assembly, configuration and break up history of Rodinia: a synthesis. *Precambrian Res.* 160, 179–210. <https://doi.org/10.1016/j.precamres.2007.04.021>.
- Lindroos, A., Romer, R.L., Ehlers, C., Alviola, R., 1996. Late-orogenic Svecocenonian deformation in SW Finland constrained by pegmatite emplacement ages. *Terra Nova* 8, 567–574.
- Linnemann, U., Pereira, F., Jeffries, T.E., Drost, K., Gerdes, A., 2008. The Cadomian orogeny and the opening of the Rheic Ocean: The diachrony of geotectonic processes constrained by LA-ICP-MS U-Pb zircon dating (Ossa-Morena and Sapo-Thuringian Zones, Iberian and Bohemian Massifs). *Tectonophysics* 461, 21–43.
- Linnemann, U., Pereira, F., Jeffries, T.E., Drost, K., Gerdes, A., 2007. The continuum between Cadomian orogenesis and opening of the Rheic Ocean: constraints from LA-ICP-MS U-Pb zircon dating and analysis of plate-tectonic setting (Saxo-Thuringian Zone, NE Bohemian Massif, Germany). *Geological Society of America, Boulder, Colorado*, pp. 61–96.
- Linnen, R.L., van Litchtervelde, M., Černý, P., 2012. Granitic pegmatites as sources of strategic metals. *Elements* 8, 275–280.
- Linnen, R.L., Cuney, M., 2005. Granite-related rare-element deposits and experimental constraints on Ta-Nb-W-Sn-Zr-Hf mineralization. *Geological Association of Canada Short Course Notes*, pp. 45–68.
- Lima, A., 2000. PhD thesis In: Estrutura, Mineralogia e Génesis dos Filões Aplitopergmatíticos com Espodumena da Região do Barroso-Alvão (Norte de Portugal). University of Porto, Portugal, and INPL, Nancy, France, pp. 270.
- London, D., 2018. Ore-forming processes within granitic pegmatites. *Ore Geol. Rev.* 101, 349–383.
- London, D., 2008. Pegmatites. *Can. Mineral. Special Publication* 10, 347.
- London, D., 2005. Granitic pegmatites – An assessment of current concepts and directions for the future. *Lithos* 80, 281–303.
- London, D., 1995. Geochemical features of peraluminous granites, pegmatites, and rhyolites as source of lithophile metal deposits. *Mineral. Assoc. Can. Short Course Handbook* 23, 175–202.
- London, D., 1992. The application of experimental petrology to the genesis and crystallization of granitic pegmatites. *Can. Mineral.* 77, 129–145.
- London, D., 1986. Magmatic–hydrothermal transition in the Tanco rare-element pegmatite: Evidence from fluid inclusions and phase-equilibrium experiments. *Am. Mineral.* 71, 376–395.
- Luecke, W., 1981. Lithium pegmatites in the Leinster Granite (southeast Ireland). *Chem. Geol.* 34, 195–233.
- Lulzac, Y., Apolinarski, F., 1986. Inventaire du territoire métropolitain les minéralisations à étain, tantale et lithium de Trégueennec (Finistère), état des connaissances au 31 mars 1986; BRGM Report 86 DAM 011 OP4, 37 p.
- Manthiram, A., Yu, X., Wang, S., 2017. Lithium battery chemistries enabled by solid-state electrolytes. *Nature Rev. Mater.* 2, 16103.
- Matte, P., 1991. Accretionary history and crustal evolution of the Variscan belt in Western Europe. *Tectonophysics* 196, 309–337.
- Matte, P., Maluski, H., Rajlich, P., Franke, W., 1990. Terrane boundaries in the Bohemian Massif; Result of a large scale Variscan shearing. *Tectonophysics* 177, 151–170.
- Marcoux, E., 2017. Mines et ressources minérales en Armorique. Société de l'industrie minérale 472 ISBN 978-2-91-835001-9.
- Marignac, C., Cuney, M., 1999. Ore deposits of the French Massif Central: Insight into the metallogenesis of the Variscan collision belt. *Miner. Deposita* 34, 472–504.
- Martín-Izard, A., Reguilón, R., Palero, F., 1992. Cassiterite U-Pb geochronology constrains magmatic-hydrothermal evolution in complex evolved granite systems: The classic Erzgebirge Tin Province (Saxony and Bohemia).
- Martínez Catalán, J.R., 1990. A non-cylindrical model for the northwest Iberian al-lochthonous terranes and their equivalents in the Hercynian belt of Western Europe. *Tectonophysics* 179, 253–272.
- Martin, R.F., De Vito, C., 2005. The patterns of enrichment in felsic pegmatites ultimately depend on tectonic setting. *Can. Mineral.* 43, 2027–2048.
- McKerrow, W.S., MacNiocaill, C., Dewey, J.T., 2000. The Caledonian orogeny redefined. *J. Geol. Soc., London* 157, 1149–1154.
- Melleton, J., Gloaguen, E., Frei, D., 2015. Rare-elements (Li-Ba-Ta-Sn-Nb) magmatism in the European Variscan belt, a review. *SGA 2015: Resources minérales dans un monde durable*, Nancy, France.
- Melleton, J., Gloaguen, E., Frei, D., Novák, M., Breiter, K., 2012. How are the emplacement of rare-element pegmatites, regional metamorphism and magmatism inter-related in the Moldanubian Domain of the Variscan Bohemian Massif Czech Republic. *Can. Mineral.* 50, 1751–1773.
- Melleton, J., Gloaguen, E., Frei, D., Lima, A., 2011. U-Pb dating of columbite–tantalite from Variscan rare-elements granites and pegmatites. *Mineral. Mag.* 75, 1452.
- Menant, A., Jolivet, L., Tuduri, J., Loiselet, C., Bertrand, G., Guillou-Frottier, L., 2018. 3D subduction dynamics: a first-order parameter of the transition from copper- to gold-rich deposits in the eastern Mediterranean region. *Ore Geol. Rev.* 94, 118–135.
- Miles, A.J., Woodcock, N.H., Hawkesworth, C.J., 2016. Tectonic controls on post-subduction granite genesis and emplacement: the Late Caledonian suite of Britain and Ireland. *Gondwana Res.* 39, 250–260.
- Mohr, S., Mudd, G.M., Giurco, D.P., 2012. Lithium resources and production: Critical assessment and global projections. *Minerals* 2, 65–84.
- Mudd, G.M., Jowitt, S.M., 2016. From mineral resources to sustainable mining – the key trends to unlock the Holy Grail. In: Proceedings of the Third AusIMM International Geometallurgy Conference (GeoMet) 2016. The Australasian Institute of Mining and Metallurgy, Melbourne, pp. 37–54.
- Müller, A., Ihlen, P.M., Snook, B., Larsen, R.B., Flem, B., Bingen, B., Williamson, B.J., 2015. The chemistry of quartz in granitic pegmatites of Southern Norway: Petrogenetic and economic implications. *Econ. Geol.* 110, 1737–1757.
- Murphy, J.B., Keppie, J.D., Nance, R.D., Dostal, J., 2010. Comparative evolution of the Iapetus and Rheic oceans: a North American perspective. *Gondwana Res.* 17, 482–499.
- Nance, R.D., Gutiérrez-Alonso, G., Keppie, J.D., Linnemann, U., Murphy, J.B., Quesada, C., Strachan, R.A., Woodcock, N.H., 2012. A brief history of the Rheic Ocean. *Geosci. Front.* 3, 125–135.
- Neace, E.R., Nance, R.D., Murphy, J.B., Lancaster, P.J., Shail, R.K., 2016. Zircon La-ICPMs geochronology of the Cornubian Batholith, SW England. *Tectonophysics* 681, 332–352.
- Nicholson, K., Anderton, R., 1989. The Dalradian rocks of the Lecht, NE Scotland: Stratigraphy, faulting, geochemistry and mineralization; *Transactions of the Royal Society of Edinburgh. Earth Sciences* 80, 143–157.
- Nironen, M., 1997. The Svecocenonian Orogen: a tectonic model. *Precambrian Research* 86, 21–44.
- Nishiyama, T., Shimoda, S., Shimosaka, K., Kanaoka, S., 1975. Lithium-bearing tsudite. *Clays Clay Miner.* 23, 337–342.
- Norton, J.J., 1973. Lithium, cesium, and rubidium—the rare alkali metals (United States Mineral Resources). USGS Professional Paper 820, 363–378.
- Novák, M., Povondra, P., 1995. Elbaite pegmatites in the Moldanubium: A new subtype of the rare-element class. *Mineral. Petrol.* 12, 159–176.
- Novák, M., Černý, P., Kimbrough, D.L., Taylor, M.C., Ercit, T.S., 1998. U-Pb ages of monazite from granitic pegmatites in the Moldanubian Zone and their geological implications. *Acta Universitatis Caroli Geologica* 42, 309–310.
- Obradović, J., Djurdjević-Colson, J., Vasic, N., 1997. Phytogenic lacustrine sedimentation – oil shales in Neogene from Serbia Yugoslavia. *J. Paleolimnol.* 18, 351–364.
- PANNN, 2017. Estudo de impacte ambiental mina da argemela; Proposta de definição de âmbito, 134 p.
- Petrik, I., Cik, S., Miglierini, M., Vaculovic, T., Dianiska, I., Ozdin, D., 2014. Alpine oxidation of lithium micas in Permian S-type granites (Gemic unit, Western Carpathians, Slovakia). *Mineral. Mag.* 78, 507–533.
- Piantone, P., Wu, X., Touray, J.C., 1994. Zoned hydrothermal alteration and genesis of the gold deposit at Le Châtelet (French Massif Central). *Econ. Geol.* 89, 757–777.
- Polgari, M., Philippe, M., Szabo-Drubina, M., Toth, M., 2005. Manganese-impregnated wood from a Toarcian manganese ore deposit, Épône mine, Bakony Mts., Transdanubia, Hungary. *Neues Jahrbuch für Geologie und Paläontologie Monatshefte* 3, 175–192.
- Raimbault, L., Burnol, L., 1998. The Richemont rhyolitic dyke, Massif Central, France: a subvolcanic equivalent of rare-metal granite. *Can. Mineral.* 36, 256–282.
- Raimbault, L., Cuney, M., Azencott, C., Duthou, J.L., 1995. Geochemical evidence for a multistage magmatic genesis of Ta-Sn-Li mineralization in the granite de Beauvoir, French Massif Central. *Econ. Geol.* 90, 548–576.
- Ramos, J.F., Ribeiro, A., Barriga, F.J.A.S., 1994. Mineralizações de metais raros de Seixão Amaral-Gonçalo (Guarda). *Bol. Minas* 31, 101–115.
- Rio Tinto Notice to ASX, Increase to Jadar Project Mineral Resources, 2 March 2017, 22 p 2017 http://www.riotinto.com/documents/170302_Increase_to_Jadar_Project_Mineral_Resources.pdf.
- Roberts, N.M.W., Slagstad, T., 2015. Continental growth and reworking on the edge of the Columbia and Rodinia supercontinents; 1.86–0.9 Ga accretionary orogeny in southwest Fennoscandia. *Int. Geol. Rev.* 57, 1582–1606.
- Roda-Robles, E., Pesquera, A., Gil-Crespo, P.P., Vieira, R., Lima, A., Garate-Olave, I., Martins, T., Torres-Ruiz, J., 2016. Geology and mineralogy of Li-mineralization in the

- Central Iberian Zone (Spain and Portugal). *Mineral. Mag.* 80, 103–126.
- Roda-Robles, E., Vieira, R., Pesquera, A., Lima, A., 2010. Chemical variations and significance of phosphates from the Fregeneda-Almendra pegmatite field, Central Iberian Zone (Spain and Portugal). *Mineral. Petrol.* 100, 23–34.
- Roda-Robles, E., Vieira, R., Lima, A., Pesquera-Pérez, A., 2009. Petrogenetic links between granites and pegmatites in the Fregeneda-Almendra area (Salamanca, Spain and Guarda, Portugal): new insights from 40Ar/39Ar dating in micas. *Estudos Geológicos* 19, 305–310.
- Romer, R.L., Kröner, U., 2015. Phanerozoic tin and tungsten mineralization – Tectonic controls on the distribution of enriched protoliths and heat sources for crustal melting. *Gondwana Res.* 31, 60–95.
- Romer, R.L., Kirsch, M., Kröner, U., 2011. Geochemical signature of Ordovician Mn-rich sedimentary rocks on the Avalonian shelf. *Can. J. Earth Sci.* 48, 703–718.
- Romer, R.L., Förster, H.J., Štěmperek, M., 2010. Age constraints for the Late-Variscan magmatism in the Altenberg-Teplice caldera (eastern Erzgebirge, Krášné hory). *Neues Jahrbuch für Mineralogie Abhandlungen* 187, 289–305. <https://doi.org/10.1127/0077-7757/2010/0179>.
- Romer, R.L., Smeds, S.A., 1997. U-Pb columbite chronology of post-kinematic Palaeoproterozoic pegmatites in Sweden. *Precambrian Res.* 82, 85–99.
- Romer, R.L., Schärer, U., Steck, A., 1996. Alpine and pre-Alpine magmatism in the root-zone of the western Central Alps. *Contrib. Mineral. Petrol.* 123, 138–158.
- Romer, R.L., Smeds, S.A., 1994. Implications of U-Pb ages of columbite-tantellites from granitic pegmatites for the Paleoproterozoic accretion of 1.90–1.85 Ga magmatic arcs to the Baltic Shield. *Precambrian Res.* 67, 141–158.
- Romer, R.L., Wright, J.E., 1992. U-Pb dating of columbite – a geochronologic tool to date magmatism and ore deposits. *Geochim. Cosmochim. Acta* 56, 2137–2142.
- Romer, R.L., Thomas, R., Stein, H.J., Rhede, D., 2007. Dating multiply overprinted Sn-mineralized granites—examples from the Erzgebirge, Germany. *Mineral. Deposita* 42, 337–359.
- Roskill Information Services Ltd., 2016. Lithium: Global Industry, Markets and Outlook to 2025. Thirteenth Edition, London.
- Rudnick, R.L., Gao, S., 2004. Composition of the continental crust. Elsevier, Amsterdam, pp. 1–64.
- Scherer, E., Mücker, C., Mezger, K., 2001. Calibration of the lutetium-hafnium clock. *Science* 293, 683–687.
- Schmid, S.M., Bernoulli, D., Fügenschuh, B., Matenco, L., Schefer, S., Schuster, R., Tischler, M., Ustaszewski, K., 2008. The Alpine-Carpathian-Dinaridic orogenic system: Correlation and evolution of tectonic units. *Swiss J. Geosci.* 101, 139–183.
- Schuster, R., Stüwe, K., 2008. The Permian metamorphic event in the Alps. *Geology* 36 (8), 303–306.
- Shengsong, Y., 1986. The hydrochemical features of salt lakes in Qaidam basin. *Chin. J. Oceanol. Limnol.* 4, 383–403.
- Silva, D., Lima, A., Gloaguen, E., Gumiaux, C., Noronha, F., Deveaud, S., 2018. Chapter 3 – Spatial geostatistical analysis applied to the Barroso-Alvão rare-elements pegmatite field (Northern Portugal). In: Teodoro, A.C. (Ed.), Frontiers in Information Systems, GIS an Overview of Applications. Bentham Science Publishers, Sharjah, UAE, pp. 67–101.
- Simić, V., Andrić, N., Životić, D., Rundić, L., 2017. Evolution of Neogene Intramontane basins in Serbia; Pre-meeting Field trip B1 Abstract, 1 p.
- Smolin, A., Beaudry, C., 2015. Mineral opportunities in Ukraine; 3rd Conference on Raw Materials. European Innovation Partnership on Raw Materials, Presentation.
- Stanley, C., Jones, G.C., Rumsey, M.S., Blake, C., Roberts, A.C., Stirling, J.A.R., Carpenter, G.J.C., Whithfield, P.S., Grice, J.D., Lepage, Y., 2007. Jadalarite, Li₂NaSiB₃O₇(OH), a new mineral species from the Jadalar Basin, Serbia. *Eur. J. Mineral.* 19, 575–580.
- Štěmperek, M., Pivec, E., Langrova, A., 2005. The petrogenesis of a wolframite-bearing greisen in the Vykmovan granite stock, Western Krášné hory pluton (Czech Republic). *Bull. Geosci.* 80, 163–184.
- Stewart, D.B., 1978. Petrogenesis of lithium-rich pegmatites. *Am. Mineral.* 63, 970–980.
- Stojadinovic, U., Matenco, L., Andriessen, P., Toljic, M., Rundic, L., Ducea, M., 2017. Structure and provenance of Late Cretaceous-Miocene sediments located near the NE Dinarides margin: Interferences from kinematics of orogenic building and subsequent extensional collapse. *Tectonophysics* 710–711, 184–204.
- Suikkanen, E., Huhma, H., Kurhila, M., Lahaye, Y., 2014. The age and origin of the Vaasa migmatite complex revisited. *Bull. Geol. Soc. Finland* 86, 41–55.
- Tarascon, J.M., 2010. Is lithium the new gold? *Nature Chemistry* 2, 510.
- Thöni, M., Müller, Ch., Zanetti, A., Habler, G., Goessler, W., 2008. Sm-Nd isotope systematics of high-REE accessory minerals and major phases: ID-TIMS, LA-ICP-MS and EPMA data constrain multiple Permian-Triassic pegmatite emplacement in the Koralpe, Eastern Alps. *Chem. Geol.* 254, 216–237.
- Thöni, M., Müller, C., 2000. Permo-Triassic pegmatites in the eo-Alpine eclogite facies Koralpe complex, Austria: Age and magma source constraints from mineral, chemical, Rb-Sr and Sm-Nd isotope data. *Schweiz. Mineral. Petrogr. Mitt.* 80, 169–186.
- Tomljenovic, B., 2002. PhD thesis. Strukturne Znacajke Medvednice i Samoborskoj gorja 208, p.
- Tourtelot, H.A., Brenner-Tourtelot, E.F., 1977. Lithium, a preliminary survey of its mineral occurrence in flint clay and related rock types in the United States. *Energy* 3, 263–272.
- Uher, P., Chudík, P., Bacík, P., Vaculovic, T., Galiova, M., 2010. Beryl composition and evolution trends: an example from granitic pegmatites of the beryl-columbite subtype, Western Carpathians, Slovakia. *J. Geosci.* 55, 69–80.
- Van Breemen, O., Bowes, D.R., Afiflou, M., Żelaźniewicz, A., 1988. Devonian tectono-thermal activity in the Sowie Gory Gneissic Block, Sudetes, Southwestern Poland: Evidence from Rb-Sr and U-Pb isotopic studies. *Ann. Societatis Geologorum Poloniae* 58, 3–19.
- Van Lichtervelde, M., Grand'Homme, A., de Saint-Blanquat, M., Olivier, P., Gerdes, A., Paquette, J.L., Melgarejo, J.C., Druguet, E., Alfonso, P., 2017. U-Pb geochronology on zircon and columbite-group minerals of the Cap de Creus pegmatites, Spain. *Mineral. Petrol.* 111, 1–21.
- Viallette, M.Y., 1963. Ages absolus par méthode au strontium des lépidolites du Massif Central français; Comptes rendus du 88ème congrès national des sociétés savantes. Clermont Ferrand, Section des Sciences, pp. 17.
- Vieira, R., Roda-Robles, E., Pesquera, A., Lima, A., 2011. Chemical variation and significance of micas from the Fregeneda-Almendra pegmatitic field (Central-Iberian Zone, Spain and Portugal). *Am. Mineral.* 96, 637–645.
- Vieira, R., 2010. PhD Thesis. Aplitopegmatitos com elementos raros da região entre Almendra (V. N. de Foz-Côa) e Barca d'Alba (Figueira de Castelo Rodrigo). Campo plítopegmatítico da Fregeneda-Almendra 275.
- Vignola, P., Diella, V., Oppizi, P., Tiepolo, M., Weiss, S., 2008. Phosphate assemblages from the Brissago granitic pegmatite, western Southern Alps, Switzerland. *Can. Mineral.* 46, 635–650.
- Vinogradov, A.P., Tugarinov, A.I., 1961. The geologic age of pre-Cambrian rocks of the Ukrainian and Baltic shields. *Ann. N.Y. Acad. Sci.* 91, 500–513.
- Yaksic, A., Tilton, J.E., 2009. Using the cumulative availability curve to assess the threat of mineral depletion: the case of lithium. *Resour. Policy* 34, 185–194.
- Yu, J., Gao, C., Cheng, A., Liu, Y., Zhang, L., He, X., 2013. Geodynamic, hydroclimatic and hydrothermal controls on the formation of lithium brine deposits in the Qaidam Basin, northern Tibetan Plateau, China. *Ore Geol. Rev.* 50, 171–183.
- Waldron, J.W.F., Schofield, D.I., White, C.E., Barr, S.M., 2011. Cambrian successions of the Meguma Terrane, Nova Scotia and Harlech Dome, North Wales: dispersed fragments of a peri-Gondwana basin? *J. Geol. Soc.* 168, 83–97.
- White, C.E., 2008. Defining the stratigraphy on the Meguma Supergroup in southern Nova Scotia; Where do we go from here? *Atlantic Geol.* 44, 58.
- Woodcock, N.H., Soper, N.J., Strachan, R.A., 2007. A Rheic cause for the Acadian deformation in Europe. *J. Geol. Soc., London* 167, 1023–1036.
- Wang, D.H., Li, P.G., Qu, W.J., Yin, L.J., Zhao, Z., Lei, Z.Y., Wen, S.F., 2013. Discovery and preliminary study of the high tungsten and lithium contents in the Dazhuyuan bauxite deposit, Guizhou, China. *Science China. Earth Sci.* 56, 145–152. <https://doi.org/10.1007/s11430-012-4504-2>.
- Zasedatelev, A.M., 1977. Quantitative model of metamorphic generation of rare-metal pegmatite with lithium mineralization: Doklady Akademii Nauk SSSR, seria geologicheskaya, Vol. 236, 219–221.
- Zelazniewicz, A., Cwojdziński, S., England, R.W., Zientara, P., 1997. Variscides in the Sudetes and the reworked Cadomian orogeny: evidence from the GB-2A seismic reflection profiling in southerwestern Poland. *Geol. Q.* 41, 289–308.
- Zhang, R., Lehmann, B., Seltmann, R., Sun, W., Li, C., 2017. Cassiterite U-Pb geochronology constrains magmatic-hydrothermal evolution in complex evolved granite systems: the classic Erzgebirge Tin Province (Saxony and Bohemia). *Geology* 45, 1096–1098.
- Zhao, G., Cawood, P.A., Wilde, S.A., Sun, M., 2002. Review of global 2.1–1.8 Ga orogens: Implications for a pre-Rodinia supercontinent. *Earth Sci. Rev.* 59, 125–162.
- Ziemann, S., Weil, M., Schebek, L., 2012. Tracing the fate of lithium—The development of a material flow model. *Resour., Conserv. Recycl.* 63, 26–34.